THE SYNTHESIS AND CHARACTERIZATION OF CESIUM $(18\text{-CROWN-6})_2$ POTASSIUM AND RUBIDIUM POTASSIUM 18-CROWN-6

By

Zheng Li

A THESIS

Submitted to
Michigan State University
in partial fulfillment of the requirements
for the degree of

MASTER OF SCIENCE

Department of Chemistry

1984

ABSTRACT

THE SYNTHESIS AND CHARACTERIZATION OF CESIUM (18-CROWN-6)$_2$ POTASSIUM AND RUBIDIUM POTASSIUM 18-CROWN-6

By

Zheng Li

The synthesis and study of the properties or two new mixed alkalide systems $Cs^+(18C6)K^-$ and RbK(18C6) are described. These salts were prepared by crystallization from solution. Analyses gave results in good agreement with the proposed stoichoimetry for $Cs(18C6)_2K$. However, in the system of Rb-K-(18C6), the originally expected compound of stoichiometry $RbK(18C6)_2$ could not be formed; instead, the complex RbK(18C6) was found. For $Cs(18C6)_2K$, the optical absorption peak of K^- at ~820 nm, the MASS-NMR peak of $Cs^+(18C6)_2$ at $\delta = 81.4$ ppm and magnetic properties confirmed that the compound was $Cs^+(18C6)_2K^-$ containing ~6% unpaired electron density, presumably doping at F-center type detects. For RbK(18C6), the preliminary studies of ^{87}Rb MASS-NMR, K-edge X-ray absorption and EPR indicated the presence of both Rb^+ and Rb^- species and the behavior of an alkalide rather than an electride. Accordingly, RbK(18C6) might be a mixed salt.

ACKNOWLEDGMENTS

I would like to express my appreciation for the assistance of many people in the researh work and the preparation of this thesis. Professor James L. Dye, my supervisor, provided guidance and useful discussion through this work. K. Mistry, M. Langer, and S. Bankroff provided prompt service for glassware. L. D. Le, N. R. Nirmala, and K. Johnson helped in the use of the NMR instrument. I am indebted to all members of this research group, M. L. Tinkham, S. Dawes, M. Faber, A. Ellabondy, O. Fussa, R. H. Huang, F. Tietega, Z. Barnes, and I. Behbahani for their cooperation and friendship.

Furthermore, I am grateful to Professor J. L. Dye and other group members, who made useful remarks about and criticisms of the thesis drafts, and to Professors H. Eick and K. Hunt who also made suggestions for revision of the manuscript.

This work was supported in part by NSF Grant Number DMR-79-21979.

TABLE OF CONTENTS

LIST OF FIGURES

LIST OF TABLES

I. INTRODUCTION

Crystalline alkalides, which contain alkali metal anions, and electrides, which consist of electrons as anions, are two new classes of ionic salts. The study of these compounds is a promising area of metal solution and solid state chemistry [1]. The present work deals with the synthesis and study of two new alkalides, $Cs^+(18C6)_2K^-$ and RbK(18C6). In this chapter, the background for the research will be reviewed. Beginning with metal solutions, the complexation of alkali metals by 18-crown-6 and the nature of alkalides and electrides will be briefly described. Next, there will be discussions of trapped electrons in condensed media and mixed alkalide-electride systems.

I.A. Solvated Electrons and Metal Anions in Solution

The investigation of alkali metal solutions originated with metal-ammonia solutions over a century ago, and extensive studies have been made [2,3]. Alkali metals are very soluble in ammonia and have characteristic colors, dark inky-blue when dilute and metallic-bronze when concentrated. The solution properties range from electronic at dilute and intermediate concentrations (<0.5 mole percent metal-MPM) to metallic in concentrated solutions (>8 MPM), with a nonmetal to metal transition occurring between 2 and 9 MPM. Very dilute metal-ammonia solutions (<0.01 M) contain solvated cations and solvated electrons. The latter are electrons equally shared among a number of molecules in the ground state [4]. As the metal concentration increases, electron-cation interactions become important. Magnetic properties show that in addition to ion-pairing between M^+ and e^-_{solv}, spin-pairing occurs to give diamagnetic states which become more predominant as the concentration increases. Candidates that have been invoked in this spin-pairing equilibrium include $e^=_2$ (two electrons in a single cavity), M^- ("genuine" metal anion), M_2 ("loose" metal dimer) and $e^-\cdot M^+\cdot e^-$ (triple ion), together with higher ionic clusters.

In less polar solvents such as amines and ethers, we expect extensive ion-pair formation to occur between M^+ and e^-_{solv}, so that the various species referred to as e^-_{solv} probably include ion-pairs or higher ionic aggregates. Golden, Guttman and Tuttle were the first to postulate the existence of "genuine" alkali metal anions in solution with two electrons in the outer s orbital [5]. The optical spectra of alkali metal-amine solution showed one main absorption band at 650-1050 nm depending on the metal and another absorption band at lower energy, 1200-2000 nm independent of the metals and solvents. EPR studies suggested that the species responsible for the higher energy absorption were diamagnetic. The high energy absorption band was then assigned to metal anions M^-, while the infrared metal-independent absorption was attributed to solvated electrons

e^-_{solv}. The conclusive proof for alkali metal anions came from the study of ^{23}Na NMR spectra [6]. The peak of Na$^+$C222 occurs at the same chemical shift as Na$^+$C222Br$^-$ in solution and that of Na$^-$ is unshifted from the value calculated for gaseous Na$^-$. The absence of a paramagnetic shift and the narrowness of the NMR line strongly support the assumption that Na$^-$ is a "genuine" anion with a highly symmetric environment. The fact that the chemical shift is independent of the solvent and is not paramagnetically shifted indicates a spherically symmetric shielding of the nucleus in the 3s orbital that prevent the 2p electrons from interacting with the solvent. Later, ^{133}Cs NMR also provided evidence for the existence of Cs$^-$ in solution [7]. Based on these observations, it is evident that alkali metal anions are the major solution species in metal amine and ether solutions.

I.B. Alkali Metal Crown Ether Systems

The synthesis of crown ethers (macrocyclic polyethers) and their ability to form stable complexes with various cations were reported by Pederson in 1967 [8]. Complexed salts of crown ethers with alkali metal thiocyanates can be crystallized from methanol [9]. The experimental results showed that dibenzo-18-crown-6 with a hole 1.4A in radius formed only a 1:1 (ligand:M$^+$SCN$^-$) complex with potassium thiocyanate ($r(K^+)=1.33$A), but that it formed no 1:1 complexes but rather 2:1 and 3:2 complexes with cesium thiocyanate ($r(Cs^+)=1.65$A). Both 1:1 and 2:1 complexes form with rubidium thiocyanate ($r(Rb^+)=1.45A$), which has a cation radius on the borderline. By analogy, the complexes of benzo-15-crown-5 can be explained in the same way, forming only a 1:1 complex with sodium and 2:1 complexes with the larger ions. Consequently, the relative size of the hole and the cation control the stoichiometry. However, it was reported that Cs^+SCN^- also forms a 1:1 complex with 18-crown-6. The structure of the 1:1 complex consists of dimers in which the two Cs^+ ions are placed, not in the hole of the crown ether, but are above the mean plane of the 18C6 and directed toward one another, bridged by two thiocyanate anions[10]. At this point, it can be argued that both ring binding sites and steric effects are important. In dibenzo-18-crown-6, replacing two CH_2CH_2-units in 18-crown-6 by two benzo-units reduces the electron density at the oxygen binding site [11]. This effect results in a marked drop in binding capacity, so only sandwich complexes of cesium are formed. Even though the sizes of the cation and ligand cavity do not restrict complex formation, they may still be major factors in governing the stability of complexes [12]. It is observed that by preferential complex formation in methanol in the presence of both K^+ and Cs^+ salts; the 1:1 complex of potassium forms in preference to the 2:1 complex of cesium, and the two salts can be separated almost quantitatively. This suggests that those cations which exactly fit the ligand cavity are bound more strongly than others. In addition, the type of solvent used also influences the complexation. For example, the formation of 1:1 or 2:1 crystalline salts of Rb^+SCN^- with dibenzo-18-crown-6 depends on the solubilities and stabilities of the components in the two solvents used. In summary, there are several factors that affect the formation of a complex.

In the early 1970's, crown ethers were used by Dye and co-workers to enhance the solubility of alkali metals in amine and ether solvents, the resulting solution containing relatively high concentrations of metal anions. These studies led to the discovery of a novel class of crystalline complexes of 18-crown-6 with alkali metals [1], named alkalides, $M^+L_nN^-$, or electrides $M^+L_ne^-$ (M and N stand for alkali metals and L for crown ethers or cryptands). It is not surprising that the formation of alkalides and electrides has similarities in cation binding to the complexation of the alkali metal thiocyanates with polyethers. Various compounds have been synthesized, such as $M(18C6)_nN$ (here N also represents e-), 1:1 (crown:cation) complexes form with Na^+, K^+, Rb^+ and 2:1 complexes form with Cs^+. $M(15C5)_nN$ gives 2:1 complexes with K^+, Rb^+, Cs^+ while $M(12C4)_2N$ yields the 2:1 complex of $K^+(12C4)_2Na^-$ [13]. However, the unusual anionic species formed in these complexes lead to distinctly new characteristics.

I.C. The Nature of Alkalides and Electrides

Ionic alkalides and electrides are formed by complexation of the cation with a non-reducible ligand, either a crown ether or a cryptand [14]. The binding energy in the crystal is mainly derived from ion-dipole interactions between the cation and the complexant as well as anion-cation attractions. Both crown ethers and cryptands complex alkali metal cations strongly enough to stabilize crystalline alkalide and electride salts. The preparation of these salts has been accomplished by three methods. The first method is to evaporate the solvent completely to yield powder with the same stoichiometry as the solution. The second is a direct deposition from the vapor of metal and complexant in the proper ratio, while the third method involves a change in solvent composition followed by gradual cooling of the saturated solution to precipitate crystals.

The crystals tend to be shiny, with characteristic colors, red, golden or bronze for most alkalides and dark-blue for electrides. These compounds are stable for long periods of time at low temperatures in vacuum or in an inert atmosphere. But they are very sensitive to air, water, light and high temperatures (in some cases, even -20°C can be a high temperature) [15,16]. Only the structure of $Na^+C222Na^-$ has been determined. It can be described as closest-packed complexed cations $(NaC222)^+$ with the charge balanced by sodium anions in the octahedral holes between the cationic layers [17]. Many attempts have been made to determine the crystal structures of other alkalides but none has been successful [1].

A general feature of the optical spectra of thin films is a major broad and asymmetric absorption band ranging from 10,000-15,800 cm^{-1} whose position depends on the anionic species (sometimes a shoulder is also observed). For alkalides, the major absorption band corresponds to the ns <—>np transition of M^-. The excited state wavefunction is therefore expected to be quite different from that of the ground state so that the transition energy depends strongly upon the particular anion being considered as well as the environment of M^-. Figure 1 shows the spectra of M^+C222M^- films, in which the dependence of the absorption maximum on the metal is similar to that of M^- in solution. However in some cases, shifts of the peak position are considerable so that it is impossible to identify the absorbing species. One example is the Na^- peak in $K^+(18C6)Na^-$ at 14,000cm^{-1}, which lies between those of K^- (12,000 cm^{-1}) and Na^- (15,400 cm^{-1}) in $Na^+C222Na^-$ and K^+C222K^- respectively. This illustrates the large effect on the absorbing species, M^- by the counter ion and the complexant. In thin films of electrides, a strong, broad absorption band at 6,000-10,000 cm^{-1} is present (sometimes in addition to the band of M^-), and the location of the absorption maximum cannot be correlated with the metal [19]. The broadness of this absorption band and the frequent appearance of a shoulder suggest that electrons can be trapped in several sites with different energies.

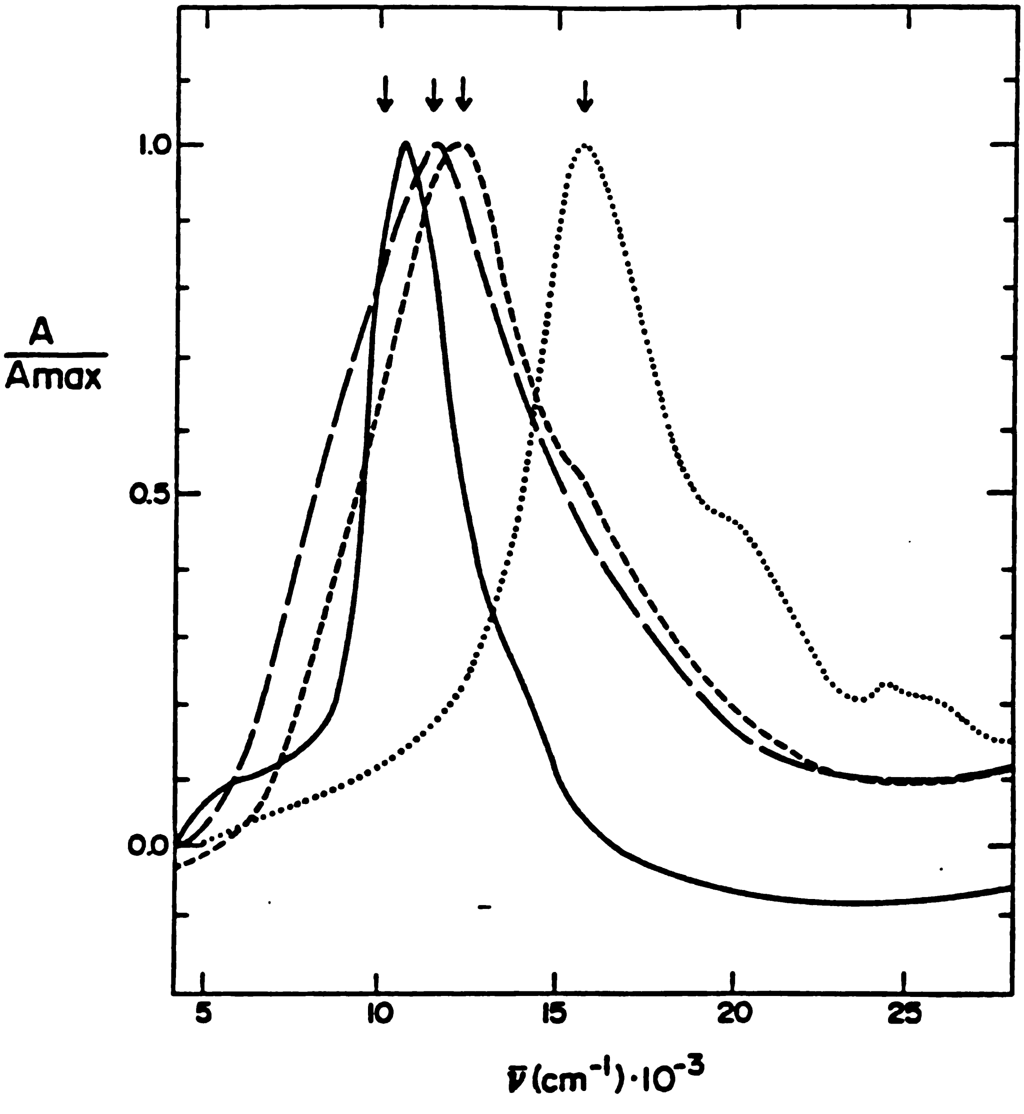

FIG. 1. Spectra of films prepared by evaporation of solutions which contain M^+C and M^-: from left to right (peak positions) M = Cs, Rb, K, Na, respectively. The arrows indicate the position of the absorption maxima for the corresponding anions in ethylenediamine.

Powder conductivity measurements of alkalides and electrides give a fairly linear relation of logσ as a function of 1/T which shows that these ionic salts behave in a similar fashion to semiconductors with band gap energies ranging from 0.8 to 2.4 ev for alkalides and 0.5 to 0.8 ev for electrides. The conductivity at infinite temperature, obtained by extrapolation of the low temperature data, indicates that a few sodides are intrinsic semiconductors while most alkalides are extrinsic semiconductors. The extrinsic behavior of alkalides probably results from electrons trapped at defect centers which dominate the thermally excited conduction process.

The study of magnetic properties provides some detailed information about the nature of the trapping sites and the interaction between electrons. Most alkalide salts show fairly strong EPR signals from trapped electrons (except $Na^+C222Na^-$, which gives a barely detectable EPR signal). The EPR spectrum of an alkalide consists of a single line with a g-value very close to that of free electrons. However, it is often broadened and becomes asymmetric due to the interaction of the electrons with the environment or because of a distribution of different trapping sites. Hyperfine splittings by Rb^+ and K^+ have been observed in $Rb^+(18C6)Na^-$ and $K^+(18C6)Na^-$ [20,21]. In these two cases, the large electron densities at the rubidium or the potassium nucleus imply that one of trapping sites is near Rb^+ or K^+. The bulk magnetic susceptibility of alkalide salts is essentially diamagnetic. A weak Curie-type paramagnetism at low temperature originates from trapped electrons. Due to the strong interaction between electrons in electrides, the magnetic properties are generally very complicated. The tendency towards spin-pairing often results in nearly diamagnetic behavior. However, the system Li-C211 exhibits striking features of temperature-dependent electron spin interactions [22]. The optical spectra of thin films confirm the presence of trapped electrons when the ratio of Li to cryptand is between 0.6 and 1.6. Electron spin resonance intensities indicate a tendency for the spins to pair as the temperature is decreased. A Curie-Weiss behavior at temperatures higher than that of the susceptibility maximum at 20-70K (depending on the ratio of Li to C211) was observed in all samples studied. From these results, it is concluded that powdered samples of Li-C211 contain nearly stoichiometric amounts of weakly interacting trapped electrons at anionic vacancies between closest-packed cryptated cations. Moreover, it is interesting that when the lithium to C211 ratio approaches two, electron delocalization occurs and the films and powdered samples behave as "expanded metals". Observations on other electride systems such as K^+C222e^- and $Cs^+(18C6)_2e^-$ confirm the complexity of such systems but have not yet provided a clear picture of the general nature of electrides. The study of electride compounds, which lie at the border line between metals and salts, is of great current interest in our research.

Magic angle sample spinning (MASS) NMR studies not only confirm the existence of the Na^- anion in sodides but also provide possible positive identification of Na^+, Na^-, Cs^+, Cs^- and Rb^- in various alkalides and electrides [23]. In ^{23}Na MASS-NMR spectra, a single narrow line of Na^- is observed at -57, -60, -63ppm respectively for $K^+(18C6)Na^-$, $Rb^+(18C6)Na^-$ and $Cs^+(18C6)_2Na^-$. The peaks of Cs^+ in $Cs^+(18C6)_2$ occur at about -60ppm in alkalides and shift paramagnetically to +81 ppm in sandwich electride samples. A line at about -300ppm corresponds to the Cs^- species [24]. The study of ^{87}Rb NMR is quite difficult because of extreme line broadening. MASS-NMR investigation of rubidium compounds are in progress.

Recent EXAFS and XANES results promise to provide identification of Rb^+ and Rb^- ions and will also provide some structural information [25].

In summary, alkalides and electrides, which contain unusual anionic species, are crystalline ionic salts with semiconducting characteristics in spite of their metallic appearance. Their properties can be altered dramatically by interactions between electrons in electrides and by the presence of non-stoichiometric electrons at F-center or other defect sites in alkalides.

I.D. F-Centers and Their Properties

One of the most important imperfections in crystals is the point defect. Such a defect can considerably alter the optical and electrical properties of materials. Furthermore, their presence is a normal thermal equilibrium phenomenon, so they can be an intrinsic feature of real crystals (also called "native defects") [26,27]. We are interested in F-center studies because they are not only a prototype of all defects but also are important in crystalline alkalides and electrides, as stated in the last section.

The F-center (also named "color center") is defined as an anion vacancy in an ionic lattice that is occupied by an electron. Studies of F-centers in alkali halides are very complete.

F-centers give colored crystals because of an absorption band of the trapped electron in the visible region. The observed absorption spectrum of an F-center consists of a broad, Gaussian-shaped absorption band. The transition (F-band) is attributed to the promotion of the trapped electrons into excited states. F-center electrons can be considered crudely as models of the "electron-in-a-box" of dimension d, which is the interionic distance. According to this model, the F-band energy corresponds to the transition from an approximate 1s ground state to a 2p excited state. The theoretical calculation predicts that the transition energy decreases as the size of the vacancy increases. In experiments, the peak positions vary from 4.97eV for LiF with the smallest lattice constant to 1.58eV for CsI with the largest interionic distance. Mollwo-Ivey also found an empirical equation for the F-center with the form

$$E_f = 17.6d^{-1.84} \qquad (1)$$

where E_f represents the energy of the absorption maximum in eV and d is the interionic distance. This relation correlated well with the theoretical model.

The presence of defects drastically changes the ability of a material to conduct electrical current. The vacancies, including F-centers and positive holes, can be described as donor or acceptor states as in semiconductors [28]. The electrons are weakly trapped at the anionic site and can be easily excited into the conduction band. A donor level is thus formed by an anion vacancy when electrons are present. Similarly, an acceptor type level can result from a cation vacancy. It is clear from an energy level picture that the defect levels occur at points within the true band gap, as indicated in Fig.2. One direct consequence of these interband energy levels is that the electrical conductivity is enhanced significantly as a function of increasing temperature. Indeed, this is just what is observed experimentally.

The F-center in alkali halides shows distinctive EPR characteristics. The g-factor is below that of free electrons and decreases with increasing interionic distance. The magnitude of the g-factor shift Δg is roughly given by

$$\Delta g \propto \lambda / \Delta E \qquad (2)$$

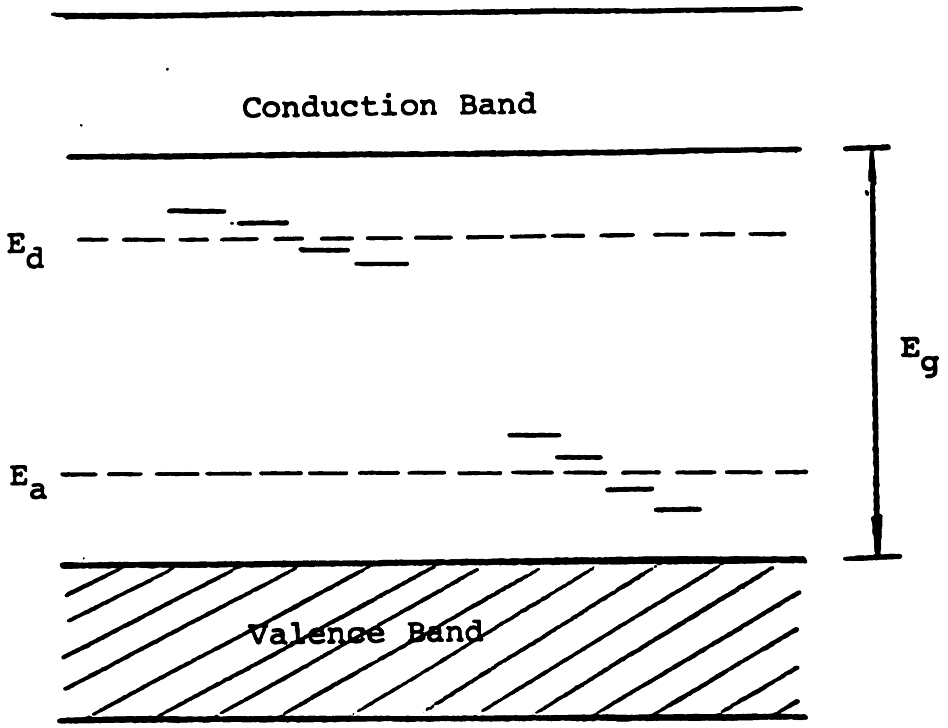

Fig.2. An energy band diagram for an ionic salt with impurities. The short bars are the impurity levels.

where λ denotes the spin-orbital coupling constant of neighboring cations and anions and ΔE is an excitation energy of electrons which may be deduced from the optical spectra. In addition, there is inhomogeneous line broadening via the hyperfine coupling with the nuclei of the salt matrix. Assuming that the F-center retains the original symmetry of the halide ion and interacts with six nearest neighbor metal cations [$2 \times 6 \times I_i$(nuclear spin quantum number)+1] lines will appear in the spectrum. Indeed, this type of hyperfine splitting has been observed in some alkali halides [29]. In practice, such a large number of hyperfine lines may overlap and the weighting factors produce a single broad resonance with approximately a Gaussian envelope. All of the available data provide a good knowledge of the nature of a F-center.

The F-center is only the simplest defect, and other more complex defect structures are also present in crystals. One important crystal defect is the Frenkel defect in which electrons are trapped at interstitial sites near a defect cation. It is also one of the possible defects in alkalides. Other examples are the M-center which is defined as two neighboring anion vacancies that bind a pair of electrons and the R-center, a type of defect that gives three adjacent F-centers. These are of particular interest in the study of trapped electrons in electrides.

I.E. Electrons in Alkali Metal-Alkali Halide Fused Salt Solutions

Liquid alkali metal-alkali halide fused salt solutions (M-MX) are examples of liquid F-centers. The solution is formed by dissolving liquid alkali metals in their alkali halide melts. Coloration occurs upon adding metal. Research began in the 1950's with the investigation of the phase diagram and electrical conductivities [30, 31]. The systems exhibited the non-metal to metal transition with increasing ratio of metal to salt (M/MX).

The primary evidence for liquid F-center is F-band absorption. The relation of the peak position with various M-MX combinations follows a modified Mollwo-Ivy equation:

$$E_m=13.0d^{-2.03} \qquad (3)$$

where E_m stands for the energy at maximum absorbance and d is the interionic distance. In comparison to the crystalline F-center data, the energies at the maximum are reduced by about 0.9ev on melting. Neutron diffraction experiments on pure alkali halides have shown that on melting no drastic changes occur in the local structure as far as the number of nearest neighbor ions is concerned. This further confirms the assumption of the F-center model in molten salts.

The EPR results also give rather direct information about the type of solvated electron states in M-MX systems [30]. The shift in the g-factor is negative and changes with the salt matrix in a way that is very similar to that observed in crystalline alkali halides. The magnitudes of the EPR spin densities suggest that in concentrated M-MX solutions an equilibrium between F-center-like defects and electrons localized in diamagnetic species (spin-pairing) has to be considered. Further support comes from the behavior of the magnetic susceptibility. It is seen that the molar susceptibility approaches the F-center value in very dilute solutions, but drops continuously with increasing metal mole fraction, x_m=0.1, near the NM-M transition region. Together with NMR studies of the dynamics of M-MX solutions, it is concluded that with increasing metal concentration, there is a continuous transformation from localized Curie-type states to spin-delocalized states, eventually approaching liquid metallic states.

The studies of the concentration and temperature dependence of optical and magnetic properties strongly support the existence of liquid F-centers at low metal concentrations and suggest that F-centers persist in equilibrium with spin-pairing aggregated centers near the NM-M transition. This special class of metal-solution brings out the differences as well as the similarities to metal-ammonia solution. The study of F-center electrons in molten salts should help to understand excess electron states in metal-solutions, and can be viewed as an example of "liquid electrides".

I.F. Mixed Alkalide-Electride Systems

Because alkalide salts are crystallized from solutions that contain solvated electrons in addition to alkali metal anions, we expect to find trapped electrons at anionic defect sites, analogous to the F-center in alkali halides.

The resulting F-center population could get rather high since electron-doping is substitutive rather than additive. In addition to electron-doping, two types of alkali anions may be formed in crystals if there is no strong preference for one over the other. Thus, salts with the formula $M^{+}L_{n}N^{-}{}_{1-y}e^{-}{}_{y}$ and $N^{+}L_{n}M^{-}{}_{1-y}e^{-}{}_{y}$ can form in mixed systems.

Susceptibility measurements of alkalides indicate that 0-5% trapped electrons can be present. Extrinsic semiconductivities are generally observed in alkalides except for a few sodides. The band gap energy obtained from conductivity studies usually does not correlate with the energy of the major absorption peak, so these salts apparently owe their conductivity to trapped electrons. The behavior of trapped electrons can be explained by the analogy to point defects in ionic salt and doped semiconductors. However, the excitation mechanism has not been fully understood. Because the observed band gap may not be the true band gap, it is described as the "apparent band gap". Photoelectron emission, which is a useful tool for the examination of band structures in solids, has been recently studied for a few sodides [33]. The data show that photoemission results from excitations of both alkali metal anions and a small fraction of trapped electrons in the sodides $Na^{+}C222Na^{-}$, $K^{+}(18C6)Na^{-}$, $Rb^{+}(15C5)_{2}Na^{-}$ and $K^{+}(15C5)_{2}Na^{-}$. In the EPR spectra, the trapped electrons show a single peak with $\Delta g \approx 0$. This indicates that electrons are trapped at sites in which they interact very weakly with the surrounding ions, perhaps at anion vacancies similar to F-centers. On the other hand, the trapped electrons that interact with the nuclei Rb^+ and K^+ show quite large hyperfine couplings, which are much greater than those observed in F-centers of alkali halides. The estimate by comparison to rubidium or potassium atoms in gas phase gives about 7-20% atomic character. This suggests that the trapped electrons which give rise to hyperfine splitting are more or less close to the cation, suggesting the presence of Frenkel-type defects. Clearly, the presence of trapped electrons may strongly influence the properties of an alkalide.

Another interesting problem is the nature of the anionic species of an alkalide when it is made from a solution that contains two different alkali metals in the presence of excess crown ether. The formation of crystals depends on the relative stability of $(ML_n)^+$ and the anion as well as the solubility in solutions. If $(ML_n)^+$ and $(NL_n)^+$ are comparable, then the resulting products may be a mixture of two crystalline compounds.

To date, most crystalline alkalides have stoichiometries of 1:1 or 2:1 (ratio of complexant to metal) and contain low concentrations of trapped electrons. By choosing appropriate starting materials, solvents and reaction conditions, it may be possible to control the complexation in order to obtain a compound with the desired stoichiometry or a mixed alkalide-electride system. The systems $Cs^+(18C6)_2Cs^-_{1-y}e^-_y$ and $Cs^+(18C6)_2Na^-_{1-y}e^-_y$ contain different extents of electron doping, some as high as 20% electron content. Whether they constitute only one type of crystal lattice or a mixture of two crystalline salts cannot be confirmed until the experimental proof of their structure is obtained. In summary, synthesis and investigation of mixed $M^+L_nN^-_{1-y}\,e_y^-$ systems will provide an opportunity to study the influence of electron density on the nature of alkalides and electrides.

II. EXPERIMENTAL

II.A. Materials

II.A.1. Metals

Potassium, rubidium (Alpha Ventron Products)and cesium (donated by the Dow Chemical Co.) were supplied under argon in sealed glass ampoules with breakseals. Total purities were 99.45% and 99.93% respectively for K and Rb according to the supplier. These metals were transferred to the distribution apparatus following the procedure outlined by D. Issa [36], then were stored under vacuum in small diameter glass tubes with sealed ends. The desired amount of the metal was obtained by measuring the length of a column of metal in a glass tube with a known inner diameter.

II.A.2. Complexing Agent

18-crown-6 (18C6 or IUPAC: 1, 4, 7, 10, 13, 16 Hexaoxacyclooctadecane, purchased from PCR Inc. or Parish chemicals) was first recrystallized from acetonitrile as the acetonitrile complex [37]. The crown ether obtained by vacuum decomposition of the acetonitrile complex, was then sublimed under high vacuum at 60°C and stored in vacuo or under an inert atmosphere in the dark.

II.A.3. Solvents

The preparation of metal solutions requires solvents that are free of reducible impurities. The purification methods are described below:

Dimthylether, DME, (Matheson, anhydrous 99.87%) was first stirred over calcium hydride at -30°C for several hours and degassed by freeze-pump-thaw cycles. It was then treated with excess Na or Na-K alloy and benzophenone until a characteristic purple-blue color formed. The purple-blue color of benzophenone ketyl served as an indicator that reducible impuries were absent. After the solution remained a stable purple-blue color for 48 hours, the solvent was distilled to a vacuum bottle and degassed again. The use of one-liter round-neck flasks and steel storage bottles made the purification more efficient. In addition, the steel bottles serve as better storage containers for volatile solvents.

Diethylether (DEE) and trimethyamine (TMA) were treated in the same way as DME.

Methylamine, MA, (Matheson) was first dried over Calcium hydride followed by degassing. The next step was to transfer the solvent to a bottle containing only Na-K alloy. Once the blue color remained for several hours, the solvent was then removed to a vacuum storage bottle and degassed by freeze-pump-thaw cycles.

II.B. Glassware

The glassware used was made of either Pyrex or fused silica. Each apparatus was equipped with a high vacuum valve designed to permit operation without diffusion of air and water vapor into the system itself. A thorough cleaning of glassware is necessary to avoid the decomposition problem. A general procedure was as follows. The apparatus was first cleaned with an HF cleaner solution (5% HF, 2% detergent, 33% HNO_3 and 60% H_2O by volume), then rinsed with distilled water. After cleaning with aqua regia, the apparatus was filled with distilled water, then conductance water (doubly deionzed) and dried in a 230°C oven for several hours.

II.C. Synthesis Procedure

The general procedure to synthesize alkalides and electrides can be divided into four stages. The apparatus for preparing samples is shown in Fig.3. The method is described here by illustrating the synthesis of $Cs(18C6)_2K$.

(1) Loading stoichiometric amounts of starting materials.

Two glass tubes, which contained equimolar amounts of Cs and K respectively, were scored and placed into the side arm. The end of the side arm was heat-sealed with Teflon shrinkable tubing which was sealed onto a closed-end glass tube. A weighed amount of 18-crown-6, equivalent to twice that of each of the metals used, was introduced through the valve or the side-arm into chamber A. The apparatus was immediately evacuated to $2x10^{-5}$ torr to prevent water absorp-

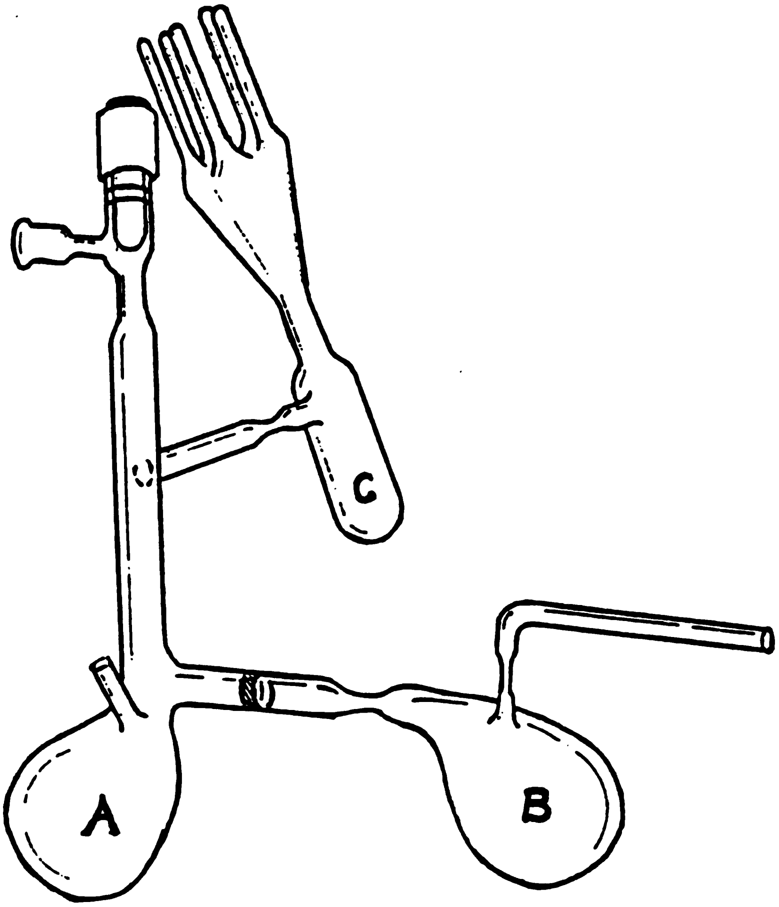

Fig.3. Apparatus for the preparation of crystalline alkalides and electrides.

tion by the crown ether. The metal-containing tubes were broken (it was necessary sometimes to cool Cs prior to breaking the Teflon tubing). Then, the metals were distilled to form a mirror in chamber B and the side arm was sealed off at the constriction.

(2) Complexation to form a stable metal-complexant solution.

The solvent bottle of DME was connected to the vacuum line. After evacuating, DME was condensed in A and the crown ether was dissolved. The system was brought to -30°C in an isopropanol dry ice bath and the solution was poured through the frit into B over the Cs-K alloy mirror. A dark blue solution formed immediately. In order to collect all of the 18C6, the blue solution was poured back and forth between chambers A and B. The apparatus was allowed to stand for a period of time with frequent shaking to dissolve the metals completely. Once all of the metals had dissolved, the solution was poured back to chamber A.

(3) Crystallization.

About half of the DME was removed and replaced with TMA, a good crystallizing solvent. Crystals were precipitated at -20°C. After warming to -5°C to give a homogeneous solution, the system was cooled down slowly to dry ice temperature -78°C, for a couple of hours. During this process, the relative amounts of the solvents were adjusted to obtain good quality crystals and to increase the yield. Finally, the supernatant liquid was poured to chamber B which was removed by freezing in liquid nitrogen and sealing off at the constriction next to the frit.

(4) Harvesting crystals.

Crystals need to be washed and stored in small sample tubes. TMA as a washing solvent was distilled into chamber A and the slurry was transferred to chamber C. The crystals were washed repeatedly with TMA and the solution was decanted into chamber A. At this point the bulk solution in A was frozen with liquid nitrogen and the crystals were dynamically pumped until they were dry. Chamber C was sealed off at the constriction, cooled and inverted to distribute crystals into sample tubes which were individually sealed off. The sample tubes were kept in a refrigerator at -78°C.

Another procedure that uses an H-cell apparatus was developed previously [1]. The whole synthesis process is simplified by the ease of the manipulation. In order to prevent the metal vapors and the solution from contaminating the vacuum valves, the H-cell has been further modified by the addition of a side-arm and extension of the necks as shown in Fig.4. In an inert atmosphere box,the tubes containing measured amounts of Cs and K were broken, placed in the side-arm and capped by a Cajon Ultra-Torr connector. Then pure 18-crown-6 was weighed and introduced into chamber B. After removal of the system from the glove box, the remaining steps were nearly the same as those described above. However, the supernatant solution after crystal-

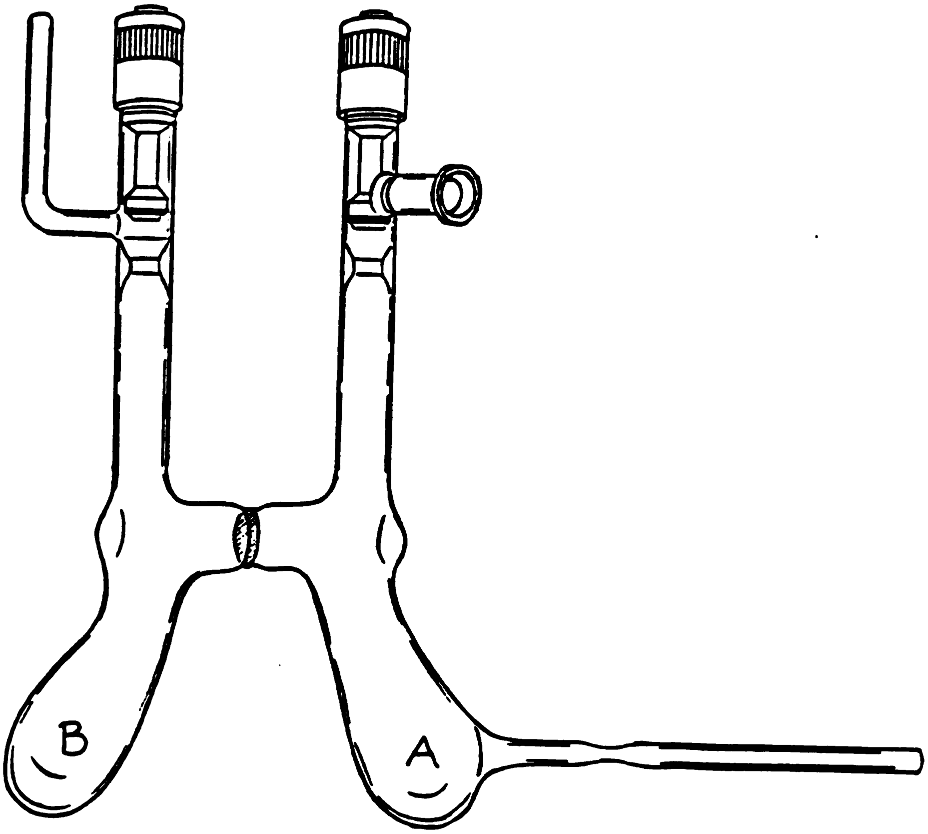

Fig.4. H-cell apparatus for the preparation of alkalides.

lization was completely removed from the H-cell into a waste vessel. The final transfer of crystals into sample tubes was handled in a glove-bag at low temperature, or in a glove-box depending on the thermal stability of the system.

II. D. Instrumental Techniques

II.D.1. Flame Emission

Flame emission was used to measure the amount of metals and gives rapid and reliable results. The instrument is a Jarrell-Ash Atomic Absorption/Flame Emission Spectrophotometer. Standard solutions of each metal in the 10-100 ppm range were prepared and used to obtain the calibration curve. The emission output value was read from a digital averager. The reading of conductance water was taken between each standard in order to give the base line correction. It was better to run the unknown sample solution following the appropriate standard solutions. Calibration curves for the standard were prepared by plotting the emission output versus concentration in ppm. The concentration of the unknown was then determined from the calibration curve. The experimental error is within ±3ppm.

II.D.2. Proton NMR

The content of cryptand or crown-ether was determined by proton NMR spectroscopy. Spectra were taken on a Bruker 250 MHz Fourier transform NMR instrument. The NMR sample was prepared by directly dissolving the dry residue [21] or crystals in D_2O, and then adding a known amount of sodium acetate as an internal standard. The ratio of crown protons to acetate protons was approximately one to one. A spectrum of a solvent free sample showed three singles; for H_2O, the crown, and the acetate protons respectively. Peaks for the crown and acetate protons were individually expanded and fitted to a Lorentzian function by a line fitting program provided by Bruker. The area under each curve was obtained by taking the product of the amplitude and the full width at half height of the curve. Based on the comparison of the areas of the crown protons and acetate protons, the number of moles of 18C6 was calculated. Furthermore, the value of the solvent content if any can also be found by ^1H NMR.

II.D.3. Optical Spectra

Spectra were taken with a Beckman DK-2 double beam recording spectrophotometer. The instrument has been modified to permit rough temperature control of the sample compartment between -80°C and 20°C by circulating cold ethanol and cooled N_2 gas. A copper-constantan thermocouple was placed in the cell compartment to measure the temperature. The optical spectra of crystalline alkalides and electrides were measured by evaporating the solvent from thin films of solutions on the inside walls of an optical cell. A typical cell used to obtain the spectra of films is shown in Fig.5. With the exception of the graded seal and the borosilcate glass vacuum valve, the apparatus was constructed from fused silica in order to avoid sodium exchange contamination of the solution by contact with sodium borosilicate glass [39]. A small amount of crystals was introduced directly from the valve into the cell inside a glove bag. After evacuating to $2X10^{-5}$ torr, MA was distilled into cell A to dissolve the crystals, giving a blue solution. The bulk solution was poured into the reservoir arm and only about 0.2 ml of the solution was left in the cell. A thin film was formed by shaking the cell vigorously in a cold isopropanol bath while the solution in the arm was frozen in liquid nitrogen. This rapid shaking splashed the solution onto the cell walls where the film formed during the flash evaporation of the solvent. It was necessary to repeat this process to obtain a film with proper thickness and uniformity.

The optical cell was placed in the cell compartment while the arm was kept in liquid nitrogen. Spectra were recorded from 4000 cm^{-1} (2500nm) to 25,000cm^{-1} (400nm) with the reference beam passing through air. The baseline was obtained by using the spectrum of an empty cell. The spectra were normalized to a scale of 0.0 to 1.0 by subtracting the baseline correction, setting the lowest absorbance to zero and the maximum to 1.0.

II.D.4. DC Conductivity

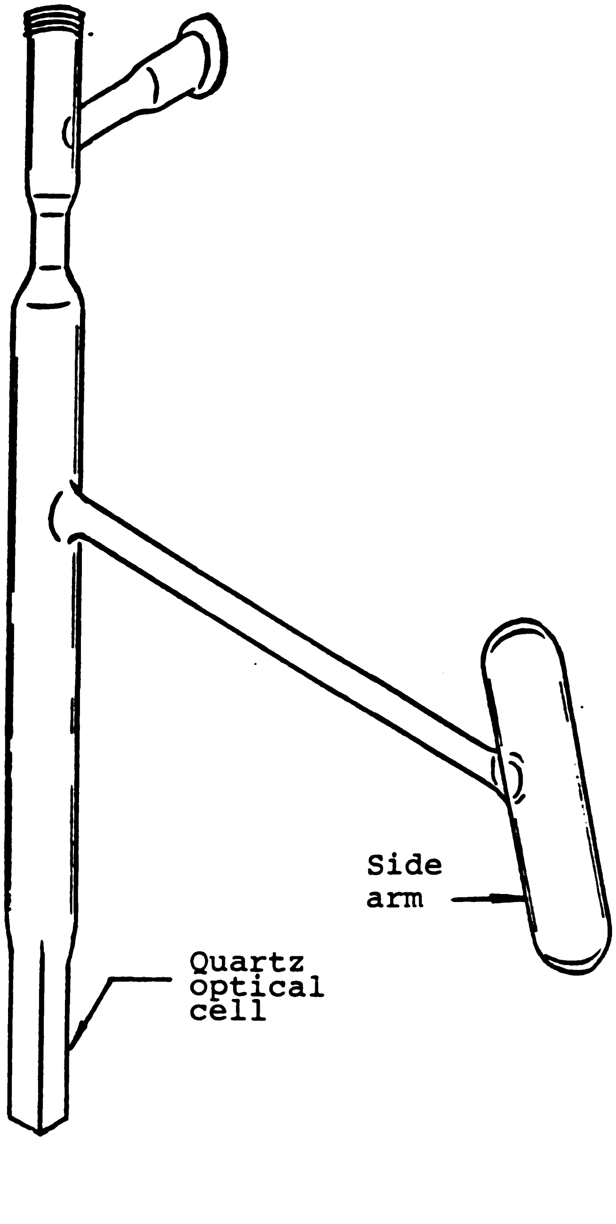

Fig.5. Apparatus for obtaining film spectra by solvent evaporation.

Because of the problems of poor quality crystals and their highly reactive nature, DC conductivity measurements were made in packed powder form by using an apparatus designed by J. L. Dye and M. R. Yemen [38]. The polycrystalline sample was loaded into a precooled 2mm ID heavy-walled quartz tube inside the glove bag. The sample tube was first placed on the bottom electrode and then the other electrode was inserted into the tube to compress the sample with a spring-loaded rod. The sample cell with the electrodes was assembled in the cryostat which was cooled by controlled liquid nitrogen boil-off. A variable temperature controller (Varian Model V-4540) was used to control the temperature over the range 160-300K.

The current through the sample as a function of applied voltage was measured with a Keithly electrometric amplifier. This permitted measurement of specific resistances up to at least 10^{10} ohm·cm. It was important to shield the conducting material of the apparatus to avoid shorts and to check if the circuit worked properly. Ohm's law obedience was tested before the measuring at a constant voltage. The reading was taken through temperature cycles. Finally, the length of the pressed powder sample was measured so that the resistivity could be estimated.

II.D.5. Electron Paramagnetic Resonance

EPR spectra were recorded on an X-band spectrometer (Bruker Model 200) over the temperature range 2-300K. The sample tube, made of quartz, was loaded in an inert environment and vacuum sealed after removal. The g-values were determined by comparison with a DPPH sample which had been calibrated against solutions of the benzene radical anion.

II.D.6. Magnetic Susceptibility

Static magnetic susceptibilities were measured with an SHE Corporation Superconducting Quantum Interference Device (SQUID). This susceptometer is capable of very precise measurements over the temperature range 1.6 to 400K. The polycrystalline sample was loaded into a Delrin bucket. During the sample transfer, the sample bucket was immersed in liquid nitrogen and introduced into the SQUID while a glove bag covered the sample introduction region to prevent the condensation of moisture. For some thermally stable samples, the loading process could be performed rapidly without using the glove bag. Measurements were taken over the temperature range 5-200K in the normal mode, and 2-5K in the 2K mode. Correction for the diamagnetism of the sample and bucket could be made by running the decomposed sample with the bucket under the same conditions. The magnetic susceptibility of the sample was calculated by taking the difference between the measured magnetization before and after decomposing the sample. The mass of the sample was determined by subtracting the weight of the empty bucket from total weight of the sample plus the bucket.

III. SYNTHESES AND ANALYSES OF $Cs(18C6)_2K$ AND RbK(18C6)

III.A. Preparation of Crystalline Samples of $Cs(18C6)_2K$

The synthesis procedure used for $Cs(18C6)_2K$ is outlined in section II.C.. The apparatus was made of Pyrex-borosilicate glass but sodium contamination was negligible. DME was used as the complexation solvent. Crystal precipitation occured almost instantly upon addition of TMA at -30°C. It was necessary to warm the system to -5°C to redissolve the crystals. The system was cooled slowly to allow slow crystallization, in order to get better quality crystals.

$\underline{Cs(18C6)_2K}$

$Cs(18C6)_2K$ samples from each preparation with initial ratios of material Cs:K:18C6=1:1:2 were identical in appearance. The deep metallic-red colored crystals were stable at room temperature for about 40 minutes so that most sample transferring and loading could be performed inside an inert atmosphere box. However, crystals readily lost their characteristic metallic-red color and turned dark blue in a few days after being exposed to an environment that contained traces of air or moisture. Under a microscope, fresh crystals appeared rod-shaped and nearly uniform in nature, although several possible products might have been formed from the starting materials.

$\underline{RbK(18C6)}$

The synthesis of equimolar Rb and K with 18C6 showed startling results. By analogy to the $Cs(18C6)_2K$ case, the starting material first was taken as Rb:K:18C6=1:1:2, since both Rb^+ and Cs^+ are too large to fit into the cavity of 18-crown-6, the expected crystal would be $Rb^+(18C6)_2K^-$. The preparation process was similar to that for $Cs(18C6)_2K$ but the precipitation of crystals was difficult, as the solution tended to form viscous metallic-bronze films on the vessel walls, rather than crystals. Crystallization of this system required the proper mixture of DME and TMA. After completely removing the solvent, two kinds of crystals with different appearances came out; one was dark-greenish and microcrystalline (nearly a powder) and the other formed as large plates with irregular square shapes covered by a thin metallic-blue film. The attempt to prepare a uniform crystalline salt of $RbK(18C6)_2$ was repeated, but the resultant products were the same.

Next, the preparation of crystalline RbK(18C6) in a 1:1:1 ratio was attempted. Crystals obtained were only dark-greenish microcrystals similar to the powder from the Rb-K-2(18C6) system. Crystals of RbK(18C6) could stand about 15 minutes at room temperature, but readily melted if warmed.

Two questions on the Rb-K-18C6 system are raised. First, what are the types of crystals in Rb-K-2(18C6); are they Rb-K-(18C6) plus excess crown? Second, what is the nature of the anion in Rb-K-(18C6)? This investigation attempted to elucidate the answers to these questions.

III.B. Analysis

The usual analytical procedure designed for alkalides and electrides was followed [41]. The analysis scheme is shown in Fig.6.

The number of reducing equivalents was first determined by decomposing a sample with water and collecting the hydrogen evolved. The number of moles of H_2 gas was calculated by using the ideal gas law. Then, the aqueous sample was titrated with standard acid solution by using a pH meter, to give an additional check of the result from H_2 evolution. These methods may give erratic results for partial decomposition may cause lower $H_2(g)$ values. Also, interaction of the 18-crown-6 with the pH electrode can give false endpoints. Flame emission was a reliable method to measure the amount of alkali metals, when the samples were diluted to appropriate concentrations of 50 ppm. The amount of 18-crown-6 was determined by ^1H NMR with NaAc as the internal reference as described by M. L. Tinkham [21].

In this study, a simpler analysis scheme was also used. The stoichiometry was determined only by sample weight, flame emission and ^1H NMR. The mass of a sample was required primarily. The number of moles of the sample was calculated from the predicted stoichiometry. Then, the sample was reacted directly with a known amount of D_2O. The solution was divided into two portions, one for the flame emission and the other for ^1H NMR. From this analysis, the

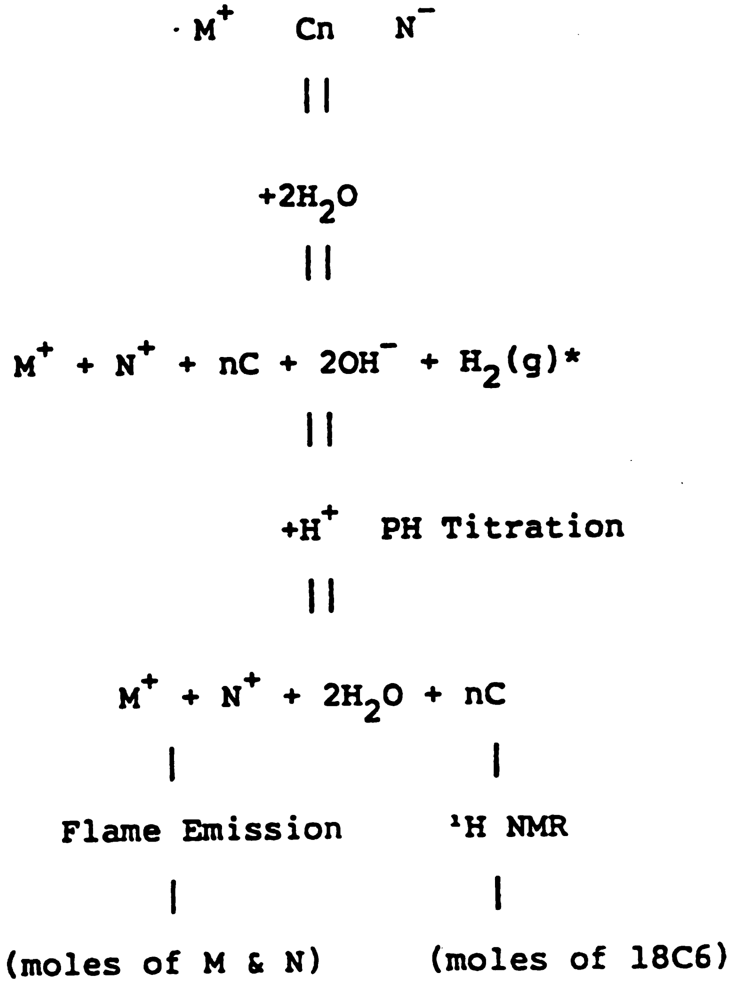

* H_2 volume gives reducing rquivalent.

Fig.6. Analytical scheme.

comparison of amounts between metal and crown gives fairly good results; also the mass of a sample was used as a reference. Furthermore, the solvent content in the crystals could be tested along with 18-C-6 analysis.

The results of both analysis schemes for $Cs(18C6)_2K$ are tabulated in Table 1. The samples were weighed on an analytical balance (Mettler AC 100) inside the glove box, thus the deviations of masses were small. In the NMR spectra with the simplified scheme, occasionally a small peak appeared adjacent to the main peak of the crown protons. This small peak was possibly caused by violent decomposition in D_2O at room temperature, yielding broken or decomposed crown ether molecules. In this case, the crown content was determined by the summation of both peaks. For all samples of $Cs(18C6)_2K$, there were no additional peaks corresponding to TMA or DME protons in the NMR spectra. Therefore, the samples were solvent free. Analysis of $Cs(18C6)_2K$ samples agreed with the presumed stoichiometry to within the estimated errors.

The analysis of the Rb-K-(18C6) system was carried out by the simplified procedure. Table 2 lists the results of the analysis. Because of the low thermal stability of the compound, the mass was estimated by weighing the sample tube before and after removing the crystals. This might result in larger error than directly weighing crystals. Analysis of crystals formed from solution of Rb-K-18C6 indicated the 1:1:1 ratio of Rb:K:18C6. This proved the exist-

TABLE 1. Results of the Analysis of Cs(18C6)$_2$K

Syn	Avg	MASS	H_2	PH	Cs^+	K^+	18C6
I	0.1015 -----	0.1016 (-)	0.1116 (+9.9)	0.2042 (+0.6)	0.0955 (-5.9)	0.0968 (-4.6)	----- -----
I*	0.1019 -----	0.09714 (-4.6)	----- -----	----- -----	0.09817 (-3.6)	0.1055 (+3.6)	0.2038 (-)
II	0.1505 -----	0.1596 (+6.0)	0.1548 (+2.9)	0.3156 (+4.9)	0.1749 (+16.2)^c	0.1143 (-24.0)^c	----- -----
II*	0.0623 -----	0.05986 (-4.0)	----- -----	----- -----	0.06185 (+6.2)	0.06114 (-1.9)	0.1282 (+2.7)

Unit: mmol.

Notes:

a) Numbers in column Avg. are the average value of the analysis data and are used as the reference.

b) The numbers in parentheses are deviation from the reference in percent.

c) The large error of metal contents of sample II was probably introduced in the dilution process.

d) The entries with an asterisk were done by the simplified analytical scheme.

ence of stoichiometric Rb-K-(18C6). Two different types of crystals in the Rb-K-2(18C6) system were separated in a glove bag by using a pair of tweezers. Due to the difficulty of the operation, the separation was not complete.

TABLE 2. Results of the Analysis of the Rb-K-18C6 System

Starting Stoi.	Avg.	MASS	Cs^+	K^+	18C6
I. RbK(18C6)	0.0653 -----	0.09069 (?)[a]	0.0598 (-8.4)	0.06481 (-0.8)	0.0713 (+9.2)
II. RbK-2(18C6)	0.05881 -----	0.05968 (+1.5)	0.05925 (+0.8)	0.06010 (+2.2)	0.1124 (-4.4)
III. Plate shaped crystal from RbK-2(18C6)	-----	0.1509	0.00883	0.00895	0.1359

Unit: mmol

Notes:

a) The loss of glass from the sample resulted in a large apparent mass of sample I.

b) The plate shaped crystals contained more than 90% 18 crown 6 and only small amounts of metals.

The plate-shaped crystals lost their color in a few minutes after opening the sealed tube. The analysis of the isolated plate-shaped crystals gave more than 90% 18C6, while the small amount of metals was due to incomplete separation. In addition, another sample from the same synthesis was analyzed and the results are consistent with the stoichiometry of starting material. If the result of the plate crystal analysis is subtracted from the total composition, the stoichiometry of the dark greenish crystal would be Rb-K-(18C6). As a result, it was preliminarily verified that the starting ratio of Rb:K:18C6=1:1:2 gave two crystals, Rb-K-(18C6) and uncomplexed 18-crown-6.

III. C. Discussion

From the starting material of Cs-K-2(18C6), it could be possible to form several salts including ceside, potasside and electrides or a mixture of these crystals. The thermodynamic calculation demonstrated that the free energy for the reaction

$$Cs(s) + K(s) + 2(18C6) \longrightarrow Cs^{+}(18C6)_2K^{-}$$

is about -11 kcal/mol [42]. This suggested that $Cs(18C6)_2K$ might be thermodynamically stable. The estimates for the compound other than the sandwich compounds were not complete. The experimental results give almost exclusively $Cs^{+}(18C6)_2K^{-}$. Therefore, we can conclude that the formation of $Cs^{+}(18C6)_2K^{-}$ is more thermodynamically favored than other products. The stability might come from both the complexation energy of the Cs^{+}-crown sandwich and the low lattice energy due to the large interionic distance.

Only the RbK(18C6) compound is formed in the Rb-K-18C6 system, the reaction when one starts with two moles of 18C6 is

$$Rb + K + 2(18C6) \longrightarrow RbK(18C6) + 18C6$$

The idea that only cesium will form sandwich compounds with 18C6 was also proposed by others. From the homogeneous solution of $RbK(18C6)_2$, crystals of the same stoichiometry could not be precipitated, even though the compound

$Rb^+(18C6)_2SCN^-$ is known [9]. The reason for this is not very clear. On the other hand, assuming Rb does not form sandwich compounds, the addition of another mole of 18-crown-6 could bring about the reaction

$$Rb + K + 2(18C6) \Longleftrightarrow Rb\cdot 18C6\cdot e + K\cdot 18C6\cdot e$$

Both electrides have been individually prepared. But the resulting crystals behaved more like alkalides than electrides.

In attempting to crystallize a compound M^+LN^- or $M^+L_2N^-$, it is desirable to prepare a solution of the same stoichiometry. The solution stoichiometry in solutions which contain two metals can be controlled by the relative stabilities of the anions and the complexed cations [1]. Indeed, $Cs(18C6)_2K$ is formed in this way. In some cases, however, the effects of lattice energy, steric repulsion of the two crown moieties and differences in ion-pair formation constants may play important roles in solid state precipitations, so that a unique compound with different stoichiometries from that of the solution is produced. Examples are the systems Rb-K-2(18C6) discussed here and 2Cs-18C6 which gave only $Cs^+(18C6)_2Cs^-$ and Cs(s) from previous work in this lab.

IV. CHARACTERIZATION

IV.A. Optical Spectra of $Cs^+(18C6)_2K^-$

The optical spectra were studied with solvent-free films from methylamine solutions containing $Cs^+(18C6)_2K^-$. The films were blue in color by transmission and red-bronze by reflection. The film spectra from samples of different preparations have the following common features: a main broad absorption with a peak at 12,200 cm^{-1} (820nm) and a pronounced shoulder at 9,000cm^{-1} (11,000nm). The position of the maximum shifted slightly to the red and the intensity of the absorption gradually decreased with increasing temperature; also the shoulder shown in Fig 7. disappeared completely in T<-20°C.

In some cases, optical spectroscopy is a good way to identify the anionic species present in a compound. For example, in this case, the position of the main absorption peak of $Cs^+(18C6)_2K^-$ films is found to be almost identical with the K^- absorption in M^+C222K^- and $K^+(18C6)K^-$ films [1]. The origin of the shoulder at 9,000 cm^{-1} may be defect electrons which are weakly trapped at anion sites. However, the absorption of Cs^-, a broad absorption at 10,500 cm^{-1} (950nm) might also contribute to the shoulder. It was considered that there is a possibility of forming Cs^- in the Cs-K-18C6 system since the complexation of the potassium cation with 18-crown-6 is much more favored than that of the

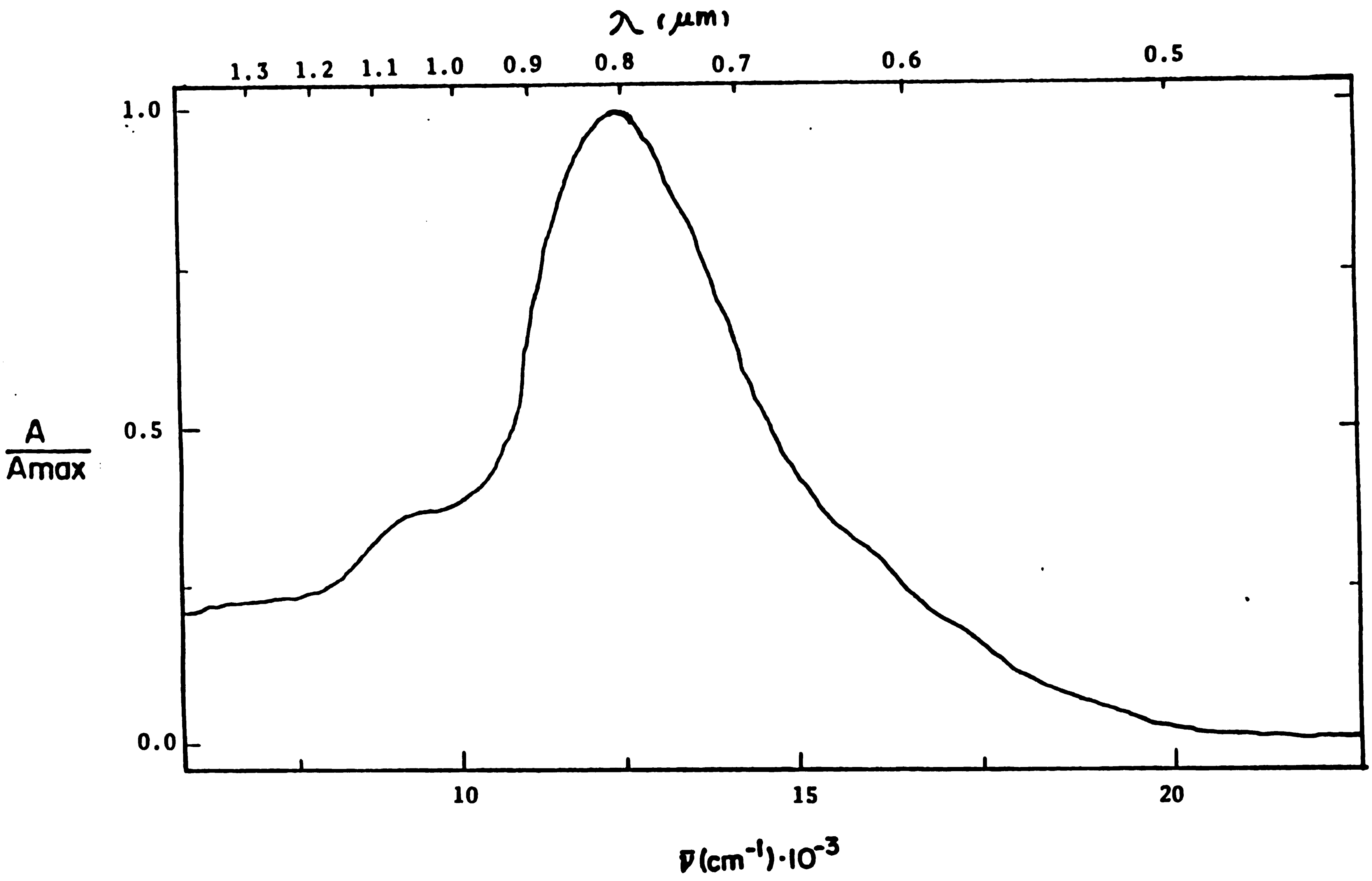

Fig.7. Optical spectrum of the thin film of $Cs(18C6)_2K$ from methylamine solution at -65°c.

cesium sandwich in solution because of the size factor. Whether Cs^- or K^- was present in the crystals was uncertain until the ^{133}Cs MASS-NMR was investigated. However, from the optical spectrum and observed stoichiometry, we could preliminarily propose that $Cs^+(18C6)_2K^-$ is a sandwich-type potasside with a small concentration of trapped electrons.

IV.B. DC Conductivity

A pressed powder sample was used to measure the DC conductivity of $Cs^+(18C6)_2K^-$. A check of the electrical circuit by measuring a standard semiconductor was performed to avoid shorts in the circuit and contact polarization effects. This was done by first loading the semiconductor TiO_2 into the sample cell. The experimental results for TiO_2 gave a band gap of 1.2ev and showed extrinsic semiconductor behavior, which is in agreement with the data taken by M. Yemen [38]. This indicated that the circuit and the assembled system were operating properly. The conductivity measurement of $Cs^+(18C6)_2K^-$ was carried out under the same conditions. First the ohmic behavior was examined by a straight line plot of current versus voltage for $Cs^+(18C6)_2K^-$ sample as shown in Fig.8. Second, the variation of the current through a temperature cycle was measured at constant voltage. Fig.9 is the plot of ln R versus 1/T over the temperature range of 215-280K. The data, taken first as the temperature was decreasing and then as the temperature was increasing, were in agreement within experimental error. Also another sample from a different preparation gave similar behavior. The apparent band gap energy was calculated from the equation

$$\sigma=\sigma_0 \exp(-E_g/2K_BT) \qquad (4)$$

Here σ_0 is the conductivity at infinite tempeature and E_g is band gap energy. Equation(4) was fit to the data by using the non-linear least squares program KINFIT [39]. The results are at as follows: the average apparent band gap is 0.88±0.03ev and the conductivities at infinite temperature range from 5 to 15 $ohm^{-1}\cdot cm^{-1}$, which indicated extrinsic behavior. Furthermore, on comparing with the optical spectrum of $Cs^+(18C6)_2K^-$, the energy of the apparent band gap of 0.88 ev is too small to correlate with the main absorption maximum at 1.6ev, but corresponds to the absorption edge at the shoulder of 1.1ev. This indicates that thermally excited electrons at defect sites are probably responsible for the observed conductivity and that the ground state of these trapped electrons lies about 0.9 ev below the conduction band. Consequently in crystalline $Cs^+(18C6)_2K^-$, trapped electrons as defect centers dominate the electrical conductivity and lead to the observed extrinsic semiconducting behavior.

IV.C. Magnetic Properties

IV.C.1. Static Magnetic Susceptibility

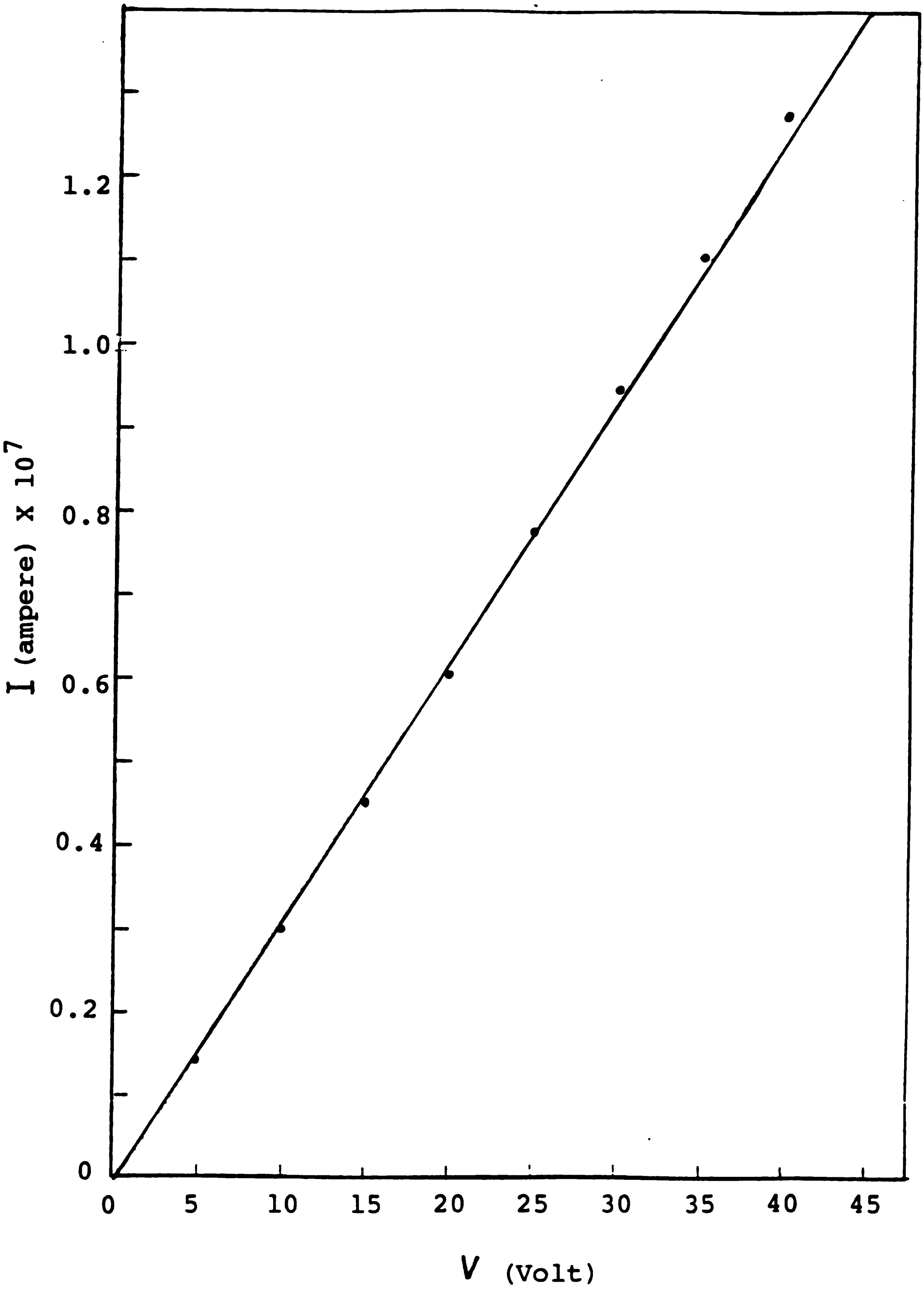

Fig.8. The I-V relation for $Cs^+(18C6)_2K^-$.

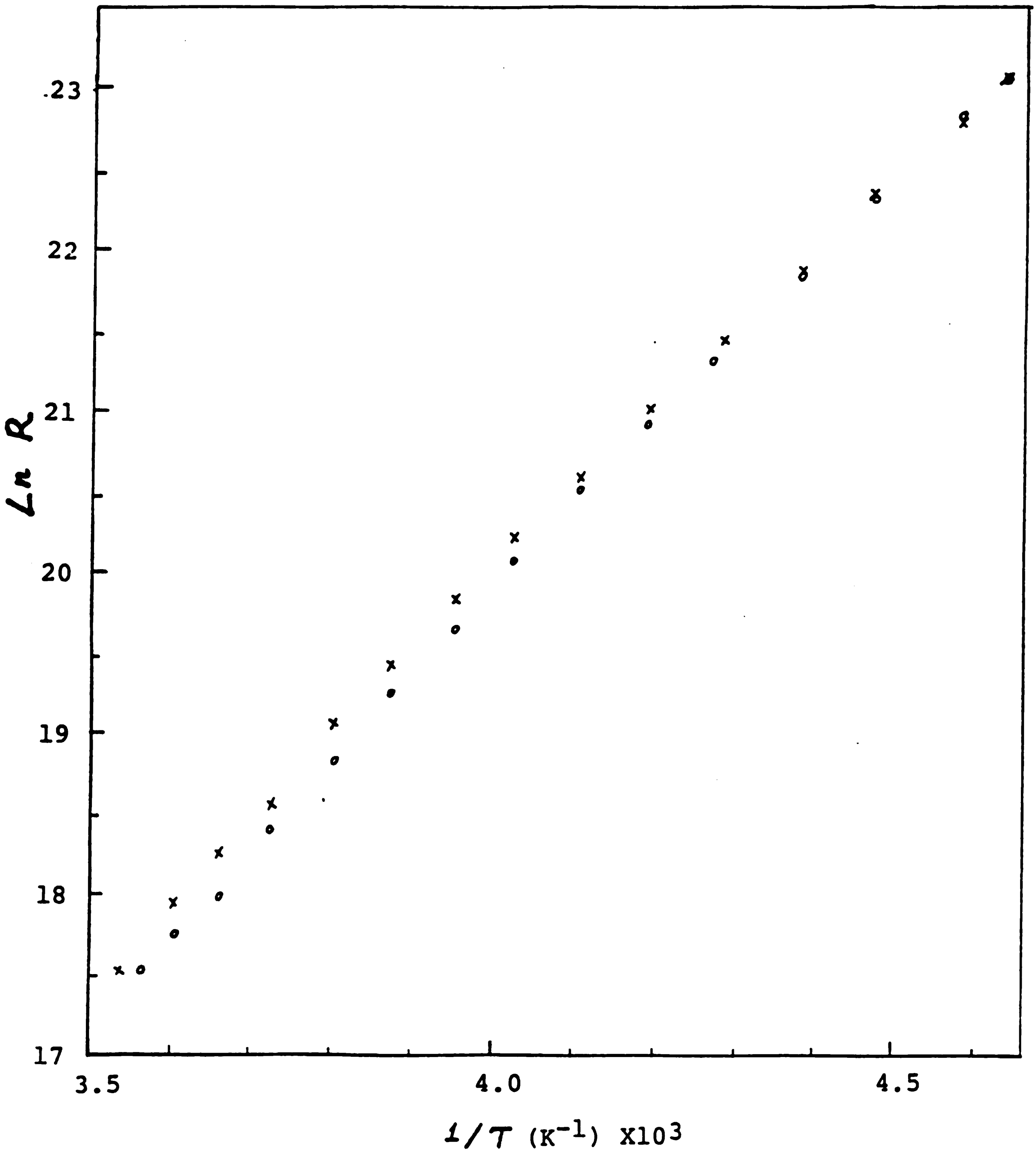

Fig.9. Log resistance vs. reciprocal of temperature for $Cs^+(18C6)_2K^-$. "x" are data taken as T increases and "o" are those for decreasing T.

The bulk magnetic susceptibility of a pure alkalide is expected to be diamagnetic due to the presence of M^- with the s^2 configuration. However, the trapped electron concentration (F-center population) could be relatively high and the electrons could be sufficiently isolated that the bulk magnetic susceptibility becomes paramagnetic.

Figure 10. shows the observed susceptibility of $Cs^+(18C6)_2K^-$ for a temperature range of 5K to 200K. There was a weak paramagnetic component of the total magnetic susceptibility which showed a tendency to continuously decrease as temperature increased as expected for Curie-type paramagnetism. Therefore, the first attempt was to fit the electronic contribution to the susceptibility by the Curie law, represented by

$$\chi_m = fC/T \qquad (5)$$

where C is the Curie constant, and f is the fraction of unpaired electrons. However, a plot of $1/\chi_m$ versus T gave a curve instead of a straight line. Thus, some interactions between the electrons and their environment in the magnetic field had to be considered. The Curie-Weiss law was then used with the addition of a diamagnetic contribution, B. The equation used is

$$\chi_m = fC/(T-\theta) + B \qquad (6)$$

in which θ is the Weiss constant. The equation was fit to the data by using the KINFIT program. The result was relatively satisfactory. The computer-fitted values of the parameters were $f=0.063\pm0.001$, $\theta=-0.9\pm0.1$ and B=

$(-5.1\pm0.7)\text{X}10^{-5}$. As expected from the Equation(6) replotting the reciprocal of (χ_m-B) vs. temperature gave a nearly linear relation at temperatures between 5K and 150K as shown in Fig.11.

The interpretation of the magnetic susceptibility of $Cs^+(18C6)_2K^-$ is as follows. Because θ is a small negative number, there might exist a very weak tendency for antiferromagnetic interactions between trapped electrons. The large negative value of the B term was initially surprising since the diamagnetic contribution from the bucket and decomposed sample had already been subtracted. However, further analysis shows that there is a difference in the diamagnetism of K^- and K^+, which cannot be cancelled in this way. It is expressed by

$$\chi=\chi_{K^-}-\chi_{K^+} \qquad (7)$$

where it is assumed that the differences between organic species before and after decomposition are negligible. The difference in the diamagnetic susceptibility of the potassium anion and cation can be estimated from the equation

$$\chi_A=-2.83\text{X}10^{10}\bullet\sum^{n}\bar{r}_i^2 \qquad (8)$$

Here, the diamagnetic susceptibility of an atom is proportional to the number of electrons, n, and the sum of the squared values of the average orbital radius $\bar{r}$ [40]. The radius of K^- is estimated to be about 3.08 angstroms [41]. Thus, the value of the diamagnetic susceptibility is calculated to be $-5.0\ \text{X}10^{-5}$ emu/mole, which is in agreement with the experimental value of the B term $-5.1\text{X}10^{-5}$. It is assumed here that two electrons initially on K^- have small effective radii in the decomposition product. In addition to that, from the value of f, the fraction of electrons is estimated to be about 6% in a mole of the $Cs^+(18C6)_2K^-$ compound. This also agrees with the proposal that F-center defects in the crystalline alkalide are essentially isolated trapped electrons and cause the paramagnetic behavior at low temperatures.

In the RbK(18C6) system, the measured electronic susceptibility had a very small positive value reduced by almost a factor of 10 in magnitude in the temperature range of 5-80K compared to that of $Cs^+(18C6)_2K^-$. There are two possibilities to explain this behavior. One is that RbK(18C6) consists largely of metal anions (either Rb^- or K^- or both) which are essentially diamagnetic and that there is only a small concentration of trapped electrons. The other is the presence of the electrides $K^+(18C6)e^-$ or $Rb(18C6)e^-$ in which strong spin-pairing could lead to a nearly diamagnetic susceptibility. More information can be obtained from the EPR study.

IV.C.2. Electron Paramagnetic Resonance

Information about trapped electrons and their microscopic environment can be obtained by Electron Paramagnetic Resonance (EPR) spectroscopy. The existence of paramagnetic species such as trapped electrons at defect centers gives rise to easily detectable EPR signals in most alkalides.

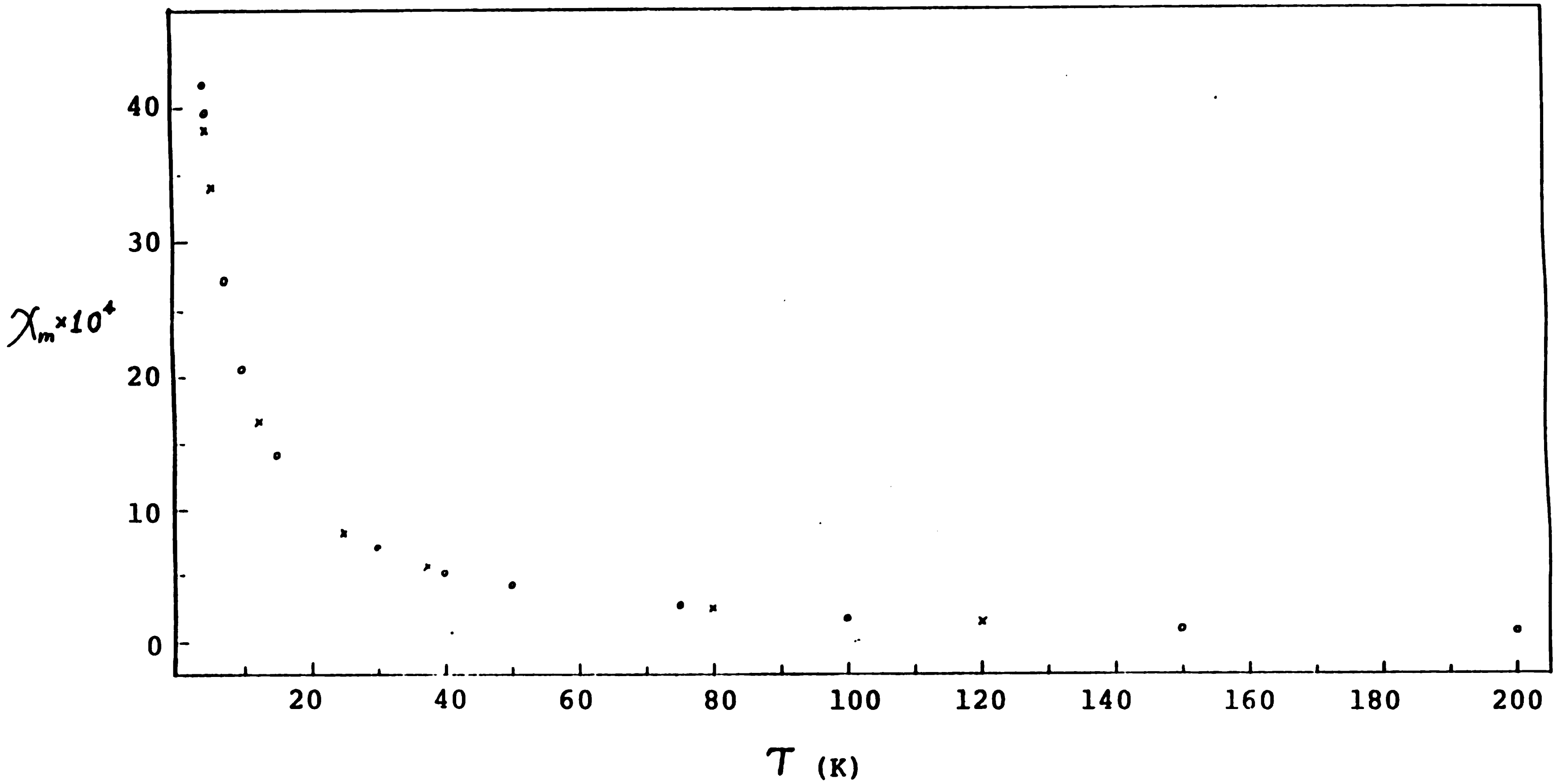

Fig.10. Dependence of static magnetic susceptibility on temperature for $Cs(18C6)_2K$ sample.

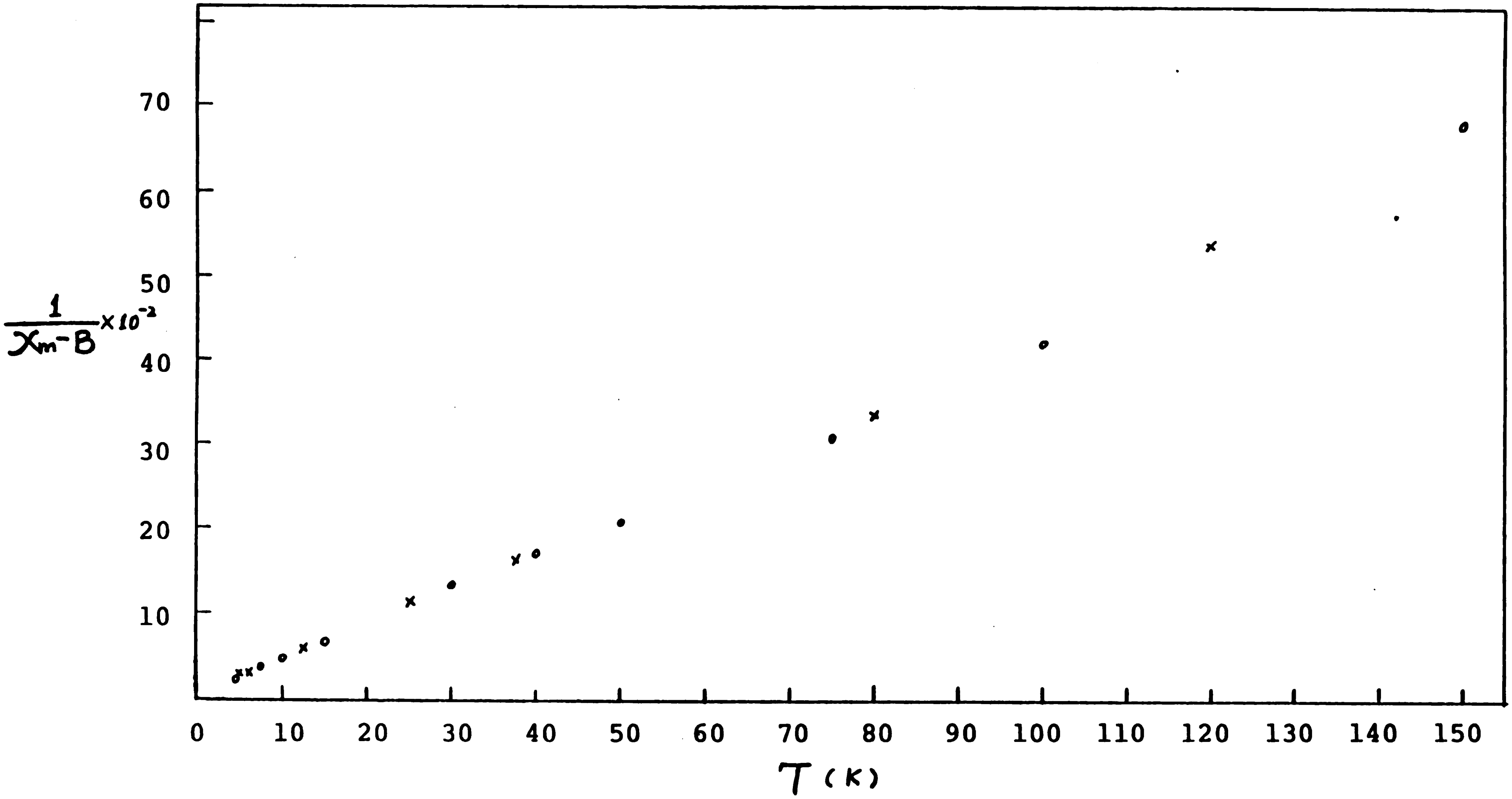

Fig.11. A plot of reciprocal (χ_m-B) as a function of temperature for $Cs(18C6)_2K$.

Because the paramagnetic electrons in alkalides and ordinary crystalline salts are embedded in the crystalline lattice, the interaction of electrons with the surroundings often results in rather complicated spectra. Some of the important effects are g-factor shifts, line broadenings and hyperfine splittings. The discussion of the EPR spectra of $Cs^+(18C6)_2K^-$ and RbK(18C6) systems in this section is based on just a few preliminary observations.

The EPR spectrum of $Cs^+(18C6)_2K^-$ has a single narrow line, of linewidth less than 1 Gauss as shown in Fig. 12. The narrowness of the line suggests rapid electron exchange, which implies a relatively high concentration of trapped electrons. No hyperfine splitting was observed in the temperature range of -100°C to -30°C, which can also be explained by rapid electron exchange. The free electron g-value implies only weak interaction between trapped electrons and the well-shielded Cs^+ sandwich complex. The preliminary conclusion is that there exist unpaired trapped electrons at a concentration that is a small fraction relative to the number of anions in crystalline $Cs^+(18C6)_2K^-$, but high enough to exchange rapidly. Moreover, the electrons are probably trapped at the rather spacious anion vacancies as F-centers with no strong interaction with neighboring ions.

In contrast, the RbK(18C6) system shows a relatively broad single EPR absorption. Figure 13 gives the EPR spectrum of RbK(18C6) with a g-value of about 2.0014 and

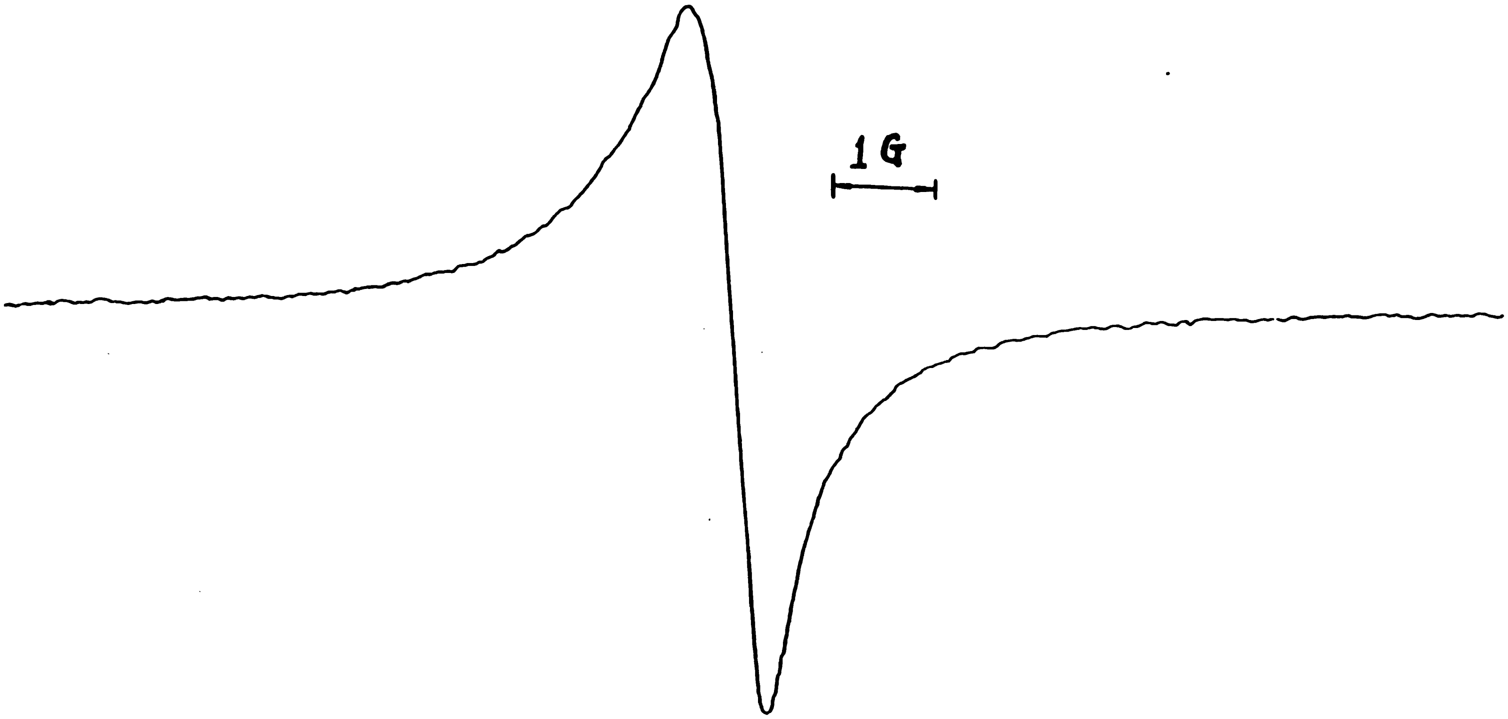

Fig.12. EPR spectra of $Cs(18C6)_2K$ at -65°C.

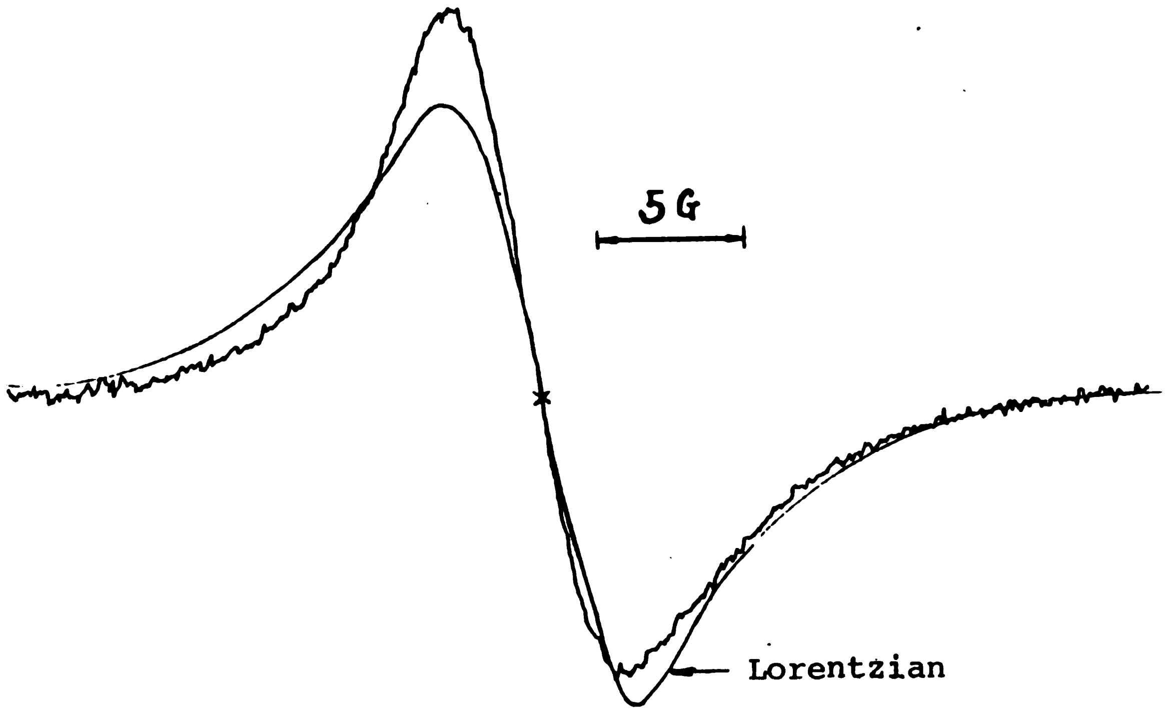

Fig.13. EPR spectra of RbK(18C6) powder at -70°C.

linewidth of about 5G. Considering that RbK(18C6) is a non-sandwich compound in which the axial position may be open, there could be substantial interactions of trapped electrons with the cations, which would broaden the line. Also, the concentration of trapped electrons is lower in this case so there would be less exchange narrowing. Hyperfine splitting might be observed at low temperatures, but this was not checked. It is shown in Fig.13. that the line shape is compatible with a Lorentzian. This indicates a nearly homogeneously broadened EPR line, which implies only a single type of electron trapping site [42]. In addition, the intensity of the EPR line is much smaller than those obtained from the electride samples (or from $Cs^+(18C6)_2K^+$). Thus, the EPR spectrum suggests that RbK(18C6) is an alkalide (perhaps mixed rubidium and potassium) with a small fraction of doped electrons present, rather than an electride. What kind of trapping site exists and how the electrons interact with the surroundings cannot be answered by this study.

IV.D. MASS-NMR of ^{133}Cs and ^{87}Rb

Since the absorbing species in thin films made from solution might differ from those present in the crystalline solid, and the peak positions can change appreciably with a change in the environment, optical spectra together with the stoichiometry cannot confirm the assignment of the species in crystalline salts. However, the measurement of the alkali metal NMR spectra in the solid state has proven to be a useful technique for identification of M^+ and M^- ionic species in alkalides and electrides. In general, the much broader NMR lines in solids, unlike those in solution, occur because of anisotropic effects such as magnetic dipole, chemical shift anisotropy and nuclear electric quadrupole interactions. To solve this problem, the Magic Angle Sample Spinning (MASS) method has been applied to the study of crystalline alkalides and electrides. The basic principle of MASS-NMR is that by rapidly rotating a solid sample at a specific angle only second order and isotropic interactions contribute to the resonance absorption. The details of such studies are described elsewhere [43,20]. By using MASS-NMR, the line width is narrowed remarkably, so that it is sometimes possible to detect the separated signal from M^+ and M^- species. To date, the MASS-NMR results have provided identification of Na^+, Na^-, Cs^+, Cs^- and Rb^- species in crystalline alkalides and electrides (as well as in the solution). The MASS-NMR spectra described here were measured by A.Ellaboudy, M.L.Tinkham and S.Dawes, and refer to the compounds $Cs^+(18C6)_2K^-$ and RbK(18C6).

The sample of $Cs^+(18C6)_2K^-$, showed only one peak at $\delta=-58$ppm in the ^{133}Cs MASS-NMR spectrum as shown in Fig.14. From the previous studies of MASS-NMR of cesium complexes $Cs(18C6)_2^+$, it was shown that the moiety in crystalline salts gave a single narrow peak at $\delta=-57 \pm 7$ppm. The one exception is the electride $Cs^+(18C6)_2e^-$, whose peak occur at

δ=+81ppm, shifted about 130 ppm. The cesium anion in $Cs^+(18C6)_2Cs^-$ has a peak at -228ppm which corresponds to Cs^- in solution at about -300ppm. From the MASS-NMR spectrum of $Cs^+(18C6)_2K^-$, neither the downfield shift of $Cs^+(18C6)_2e^-$ nor the upfield shift of Cs^- was observed. This confirms the presence of only the $Cs^+(18C6)_2$ complex. Thus, Cs(18C6)K is the cesium sandwich potasside.

^{87}Rb MASS-NMR studies are currently in progress in this laboratory. Rb^+ signals have only been observed in model rubidium salts and those from Rb^- in two alkalides $Cs^+(18C6)_2Rb^-$ and RbK(18C6). The ^{87}Rb MASS-NMR spectrum of the RbK(18C6) system is shown in Fig.15. There are two weak peaks very close together at -185 and -194ppm. $Cs^+(18C6)_2Rb^-$ whose composition has been comfirmed as $Cs^+(18C6)_2Rb^-$ by ^{133}Cs NMR gives a strong peak at -193ppm. These peak positions are nearly consistent with the Rb^- signal observed in solutions [20]. It was found that the intensities of the peaks in RbK(18C6) were much smaller than those in $Cs^+(18C6)_2Rb^-$ for the same number of scans. This indicates a low concentration of the Rb^- ion in RbK(18C6). In addition, the presence of two peaks implies two different sites for the Rb^- ion. Therefore, these results suggest that the compound RbK(18C6) is likely to be a mixture of $K^+(18C6)Rb^-$ and $Rb^+(18C6)K^-$ as well as perhaps $Rb^+(18C6)Rb^-$ and $K^+(18C6)K^-$. A final conclusion can not be made until structural information and the identification of the potassium species are obtained.

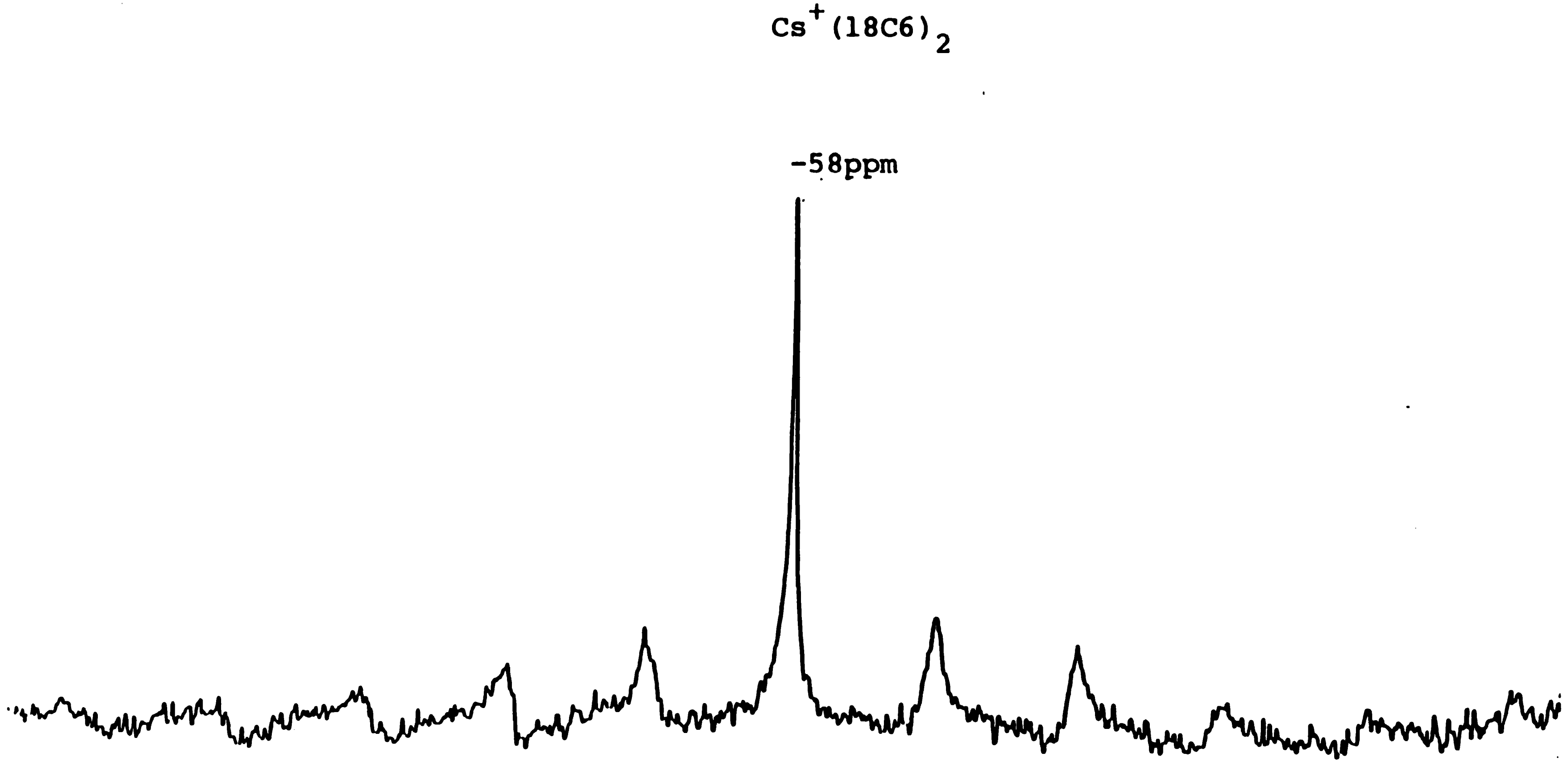

Fig.14. ^{133}Cs MASS-NMR spectrum of $Cs(18C6)_2K$.

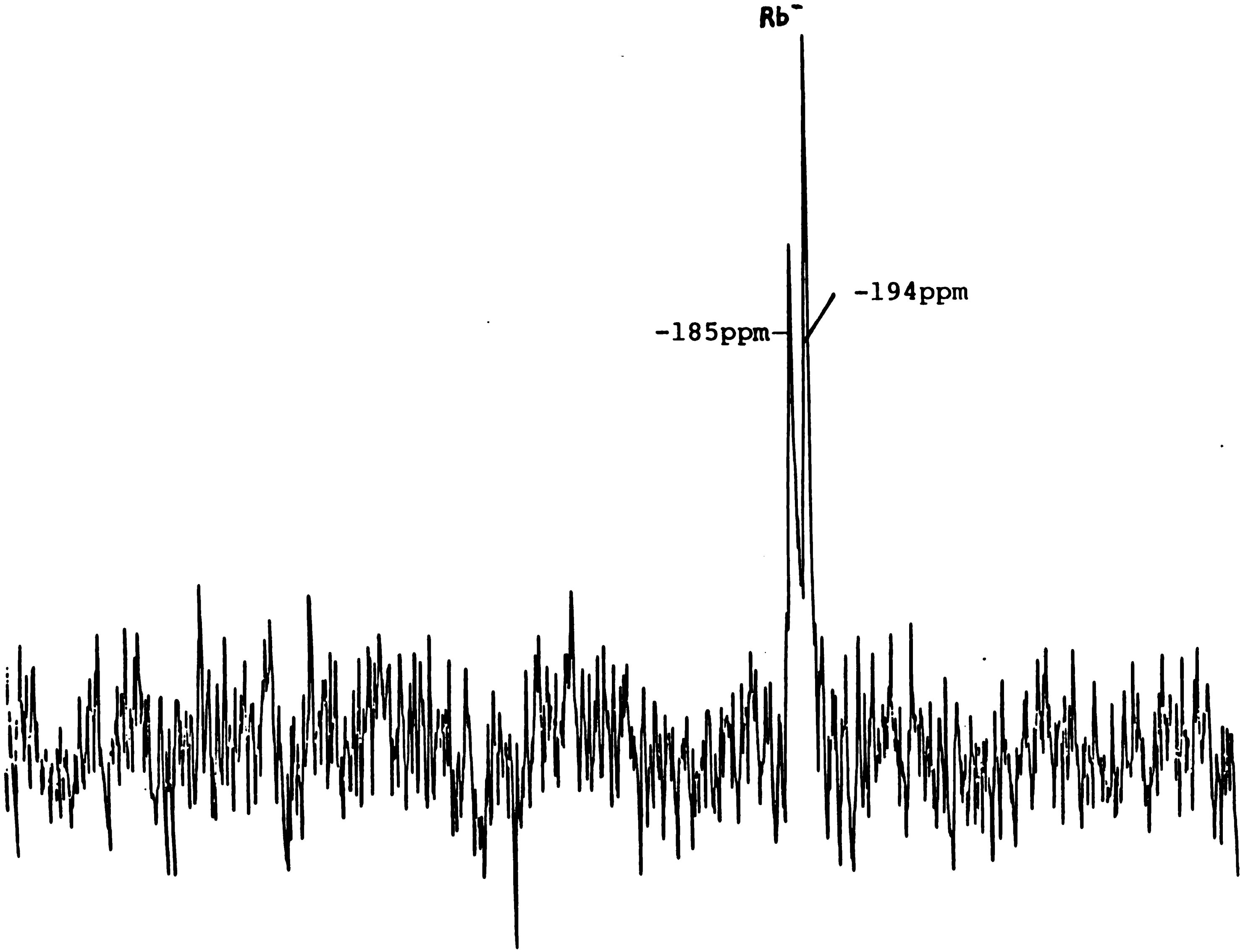

Fig.15. ^{87}Rb MASS-NMR spectrum of RbK(18C6).

IV.E. XANES and EXAFS Study of RbK(18C6)

Extended X-ray absorption fine structure (EXAFS) and X-ray absorption near edge structure (XANES) have become powerful structural tools. From a quantitative view, the probability that an X-ray photon will be absorbed by a core electron depends on both the initial and the final state of the electron. In K-edge absorption, the initial state is the 1s level and the final state can be either a bound electronic state of the absorbing atom or an emitted photoelectron. Because the absorbing atom in a molecule or in a condensed phase is surrounded by neighboring atoms, electron donation into vacant orbitals can give rise to different absorption threshold resonances near the K-edge. Also backscattering of the emitted photoelectron gives rise to an absorption coefficient u versus energy E, which displays a complex fine structure. These two features are the basic properties of XANES and EXAFS [44].

In the identification of oxidation states for the rubidium as Rb^+ or Rb^- in crystalline compounds, of particular interest is to observe the differences near the K-edge (XANES) in terms of the intensity of the "white line", since the final bound states of Rb^+ and Rb^- cannot be the same. The model salt $Rb^+(18C6)Br^- \cdot 2H_2O$ has a white line with a relatively large area. This implies a high density of vacant bound states involved in the transition. In contrast, the XANES for $Cs^+(18C6)_2Rb^-$ showed a much smaller white line area, indicating free atom-like absorption similar to that for the gaseous Kr [25]. Therefore, compounds that give a large white line area are those containing Rb^+ ions. Among all the compounds studied, the smallest area of the white line occurred in a $Cs^+(18C6)_2Rb^-$ sample which has been characterized as a rubidide by its properties and ^{133}Cs and ^{87}Rb MASS-NMR [25]. In this view, the white line area of the rubidium model salt $Rb^+(18C6)Br^- \cdot 2H_2O$ and nearly pure rubidide $Cs^+(18C6)_2Rb^-$ were taken as the references for Rb^+-18-crown-6 complex and Rb^- respectively. The investigation was done by comparing the size of the white line for various salts under study.

The XANES and EXAFS spectra were taken by Odette Fussa. The following is a brief discussion of the results for the RbK(18C6) compound. Fig. 16 gives the spectra of the reference compounds $Rb^+(18C6)Br^- \cdot 2H_2O$ and $Cs^+(18C6)_2Rb^-$, and Fig. 17 is the X-ray absorption spectrum of a sample of RbK(18C6). It is seen that the size of the white line of the RbK(18C6) sample is between those of pure $Rb^+(18C6)$ and pure Rb^-; furthermore, the magnitude of the Fourier transform of the peak for the Rb^+ complex is also intermediate between those of the reference compound data. Thus, the X-ray absorption results suggest the presence of both Rb^+ and Rb^- species in crystalline RbK(18C6). As discussed in the section on MASS-NMR studies the pure rubidide could not be ruled out, but the NMR intensity suggested a mixture of rubidide and potasside. The EXAFS and XANES studiies fur-

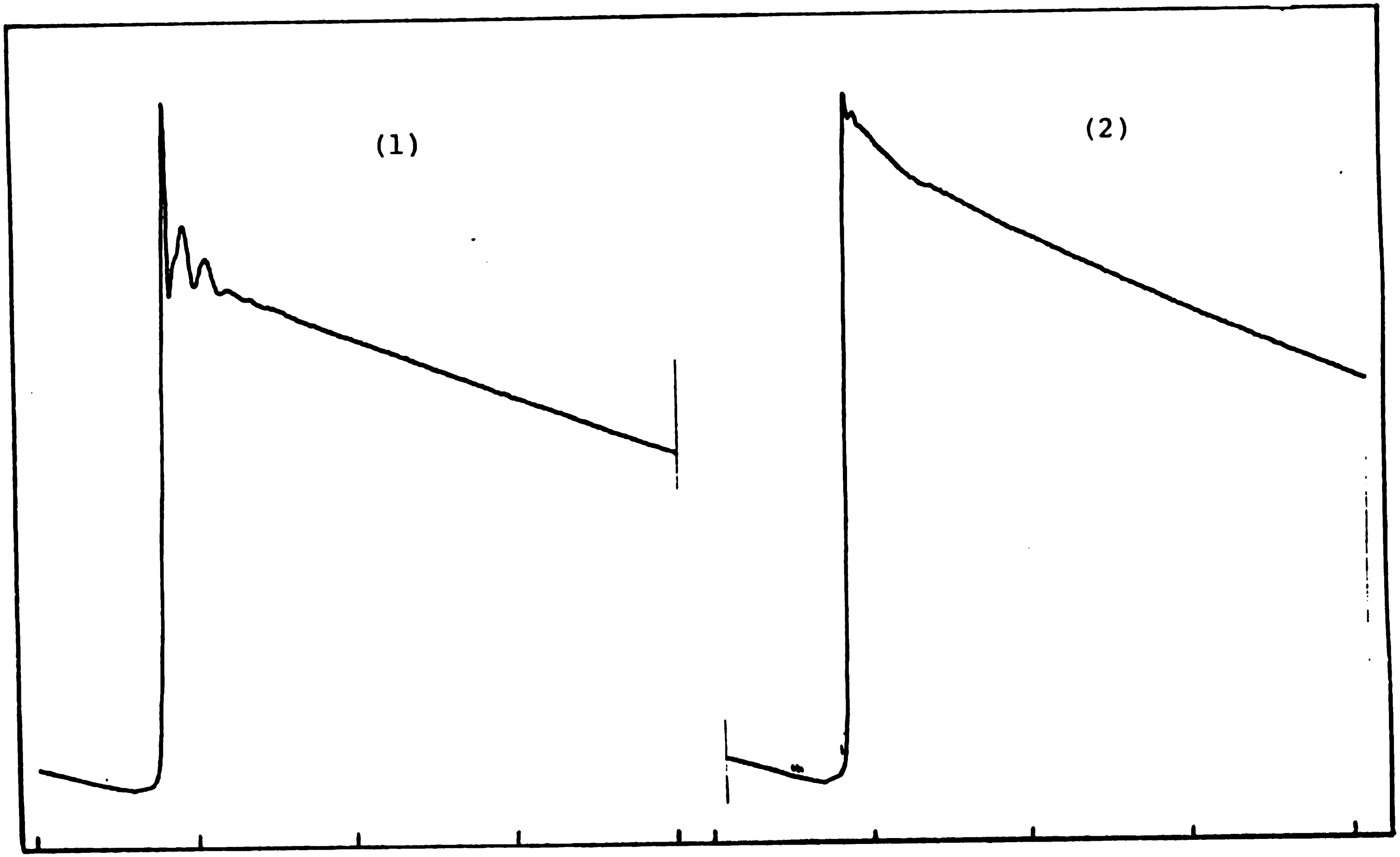

Fig.16. The X-ray spectra of $Rb^{+}(18C6)Br^{-} \cdot 2H_2O$(1) and $Cs^{+}(18C6)_2Rb^{-}$(2)

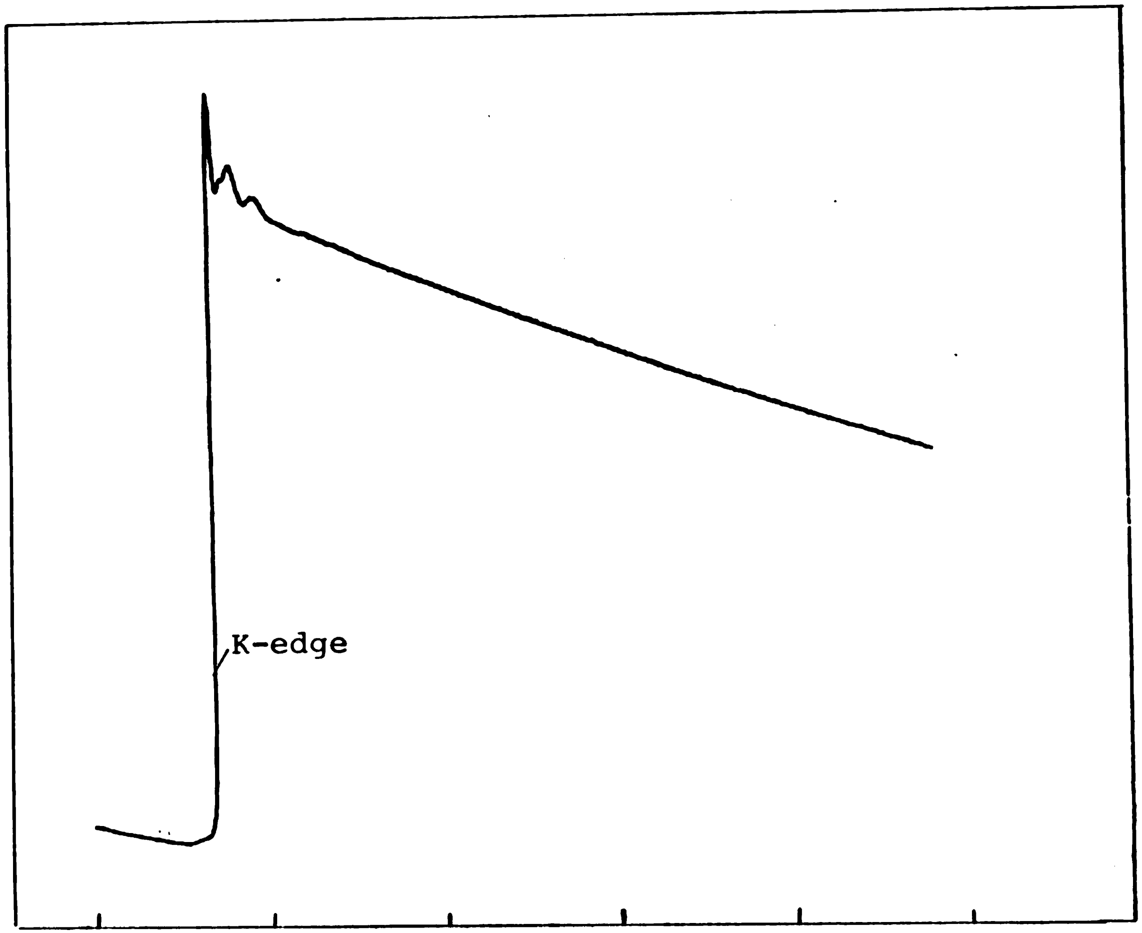

Fig.17. The X-ray spectrum of RbK(18C6) sample.

ther support the assumption that the salt of stoichiometry RbK(18C6) is a mixture of K^+(18C6)Rb^- and Rb^+(18C6)K^-. Of course, we might also expect the presence of K^+(18C6)K^- and Rb^+(18C6)Rb^-.

V. CONCLUSIONS AND SUGGESTIONS FOR FURTHER WORK

V.A. Conclusions

$Cs(18C6)_2K$

On the basis of this study, the crystalline salt of stoichiometry $Cs(18C6)_2K$ is clearly characterized as a cesium sandwich 18-crown-6 complex potasside $Cs^+(18C6)_2K^-$ containing a small fraction of trapped electrons as F-center defects. The assignment of the ionic species was suggested by the optical spectrum of films and proved by ^{133}Cs MASS-NMR studies. The optical spectrum shows an absorption band at 12,000cm^{-1} for K^- and a shoulder at 9,000cm^{-1} for trapped electrons. It appears to be an extrinsic semiconductor with an apparent band gap of 0.88 eV, which probably results from trapped electrons. The magnetic susceptibility measurement demonstrates a weak Curie-Weiss type paramagnetism and gives approximately 6% unpaired spins. Likewise, the EPR study confirms the presence of electrons as F-center defects. It is evident that the trapped electrons play a key role in the electrical and magnetic characteristics of the the compound. Moreover, the thermal stability of $Cs(18C6)_2K$ is relatively high among potasside systems and is comparable to that of sodides. Crystals of $Cs^+(18C6)_2K^-$ may be also good candidates for recrystallization in order to grow high quality single crystals for structural and other investigations.

RbK(18C6)

Syntheses with starting compositions of Rb-K-2(18C6) and Rb-K-(18C6) have been made. The preliminary analyses show that the resulting complexed crystals are the same and have the stoichiometry RbK(18C6), whether or not excess crown is present during synthesis. ^{87}Rb MASS-NMR and XANES spectra indicate that it contains both the Rb^+(18C6) complex and the Rb^- ion. A weak broad signal in the EPR spectrum together with nearly diamagnetic behavior, similar to the features of other alkalides, suggests that the sample contains alkalide ions with a small fraction of paramagnetic species, such as unpaired electrons. Although RbK(18C6) has not been completely characterized, the experimental results we have so far permit us to propose that RbK(18C6) is likely to be a mixture of $Rb^+(18C6)K^-$, $K^+(18C6)Rb^-$, $Rb^+(18C6)Rb^-$ and $K^+(18C6)K^-$.

V.B. Suggestions for Further Work

(1). To grow suitable single crystals of $Cs(18C6)_2K$ by recrystallization is indispensable for structure determination and would be very useful for studies of single crystal conductivity and EPR spectra. A study of the photoconductivity and photoemission should be performed in order to reveal the true band gap and electronic states in the system. To understand the nature of potassides and excess electrons at defect sites, attempts should be made to obtain more detailed information, and quantitative data if possible. This salt is the first stable potasside and very little is known about about the nature of such alkalides.

(2). Both the analysis and characterization of the RbK(18C6) system are primitive and need to be extended. Optical spectra and DC conductivity measurements should be done to further elucidate the nature of the anionic species. There is also a need to grow single crystal of RbK(18C6). This may help to determine whether the compound is a mixed-alkalide or a mixture of crystals such as Rb(18C6)K, K(18C6)Rb, Rb(18C6)Rb and K(18C6)K. Perhaps only the most stable of these crystals would form if slowly grown.

(3). The syntheses of other similar alkalides or mixed systems should be further explored. The approach would be to change solvents, use various complexants and choose different ratios of metal to complexant. This would also provide information about complex formation and the relative stability of various complexes.

VI. REFERENCES

[1] J.L.Dye, "Progress in Inorganic Chemistry", Vol.32, (1983).

[2] J.J.Langowski and M.J.Sienko, (eds.), "Metal-Ammonia Solutins", Bterworths, London, 1970.

[3] J.C.Thompson, "Electrons in Liquid Ammonia", Clarendon Press, Oxford, 1976.

[4] J.Jortner and N.R.Kenstner(eds.), "Electrons in Fluids", Springer-Verlag, New York, 1973.

[5] I.Hurley, T.R.Tuttle, Jr.and S.Golden, J.Chem.Phys., 48, 2818(1968).

[6] M.T.Lok, F.J.Tehan and J.L.Dye, J.Phys.Chem., 76, 2975(1972).

[7] J.M.Ceraso, and J.L.Dye, J.Am.Chem.Soc., 96, 7203 (1974).

[8] C.J.Pederson, J.Am.Chem.Soc., 89, 7017(1969).

[9] C.J.Pederson, J.Am.Chem.Soc. 92, 386(1970).

[10] J.L.Dye, J.Pure and Appl.chem., 49, 3(1977).

[11] F.de Jong and D.N.Retnbondt, "Stability and Reactivity of Crown Ether Compounds".

[12] J.D.Lamb, R.M.Izatt, C.S.Swain, and J.J.Christensen, J.Am.Chem.Soc., 102, 475(1980).

[13] M.L.Tinkham, to be published.

[14] M.Dobler and R.P.Phizackerley, Acta.Cryst., B30, 2748(1974).

[15] J.M-Lehn, J.P.Sauvage, and S.Dietrick, J.Am.Chem.Soc., 92, 2916(1970).

[16] B.Van Eck, L.D.Le, D.Issa and J.L.Dye, Inorg.Chem. 21, 1966(1982).

[17] M.H.Cohen, J.Jortner, and J.C.Thompson, J.Chem.Phys., 63, 3741(1975).

[18] F.J.Tehan, B.L.Barnett and J.L.Dye, J.Am.Chem.Soc., 96, 7203(1974).

[19] J.L.Dye, M.R.Yemen and M.G.DaGue and J-M Lehn, J.Chem. Phys., 68, 1665(1978).

[20] A.Ellaboudy, Ph.D.Dissertation, Michigan State University, 1982.

[21] M.L.Tinkham, M.S.Thesis, Michigan State University, 1982.

[22] J.S.Landers, J.L.Dye, A.Stacy and M.J.Sienko, J.Phys.Chem., 85, 1096(1981)

[23] A.Ellaboudy, M.L.Tinkham, S.Dawes and J.L.Dye, to be published.

[24] J.L.Dye and A.Ellaboudy, Chem.in Britain, 20, 210 (1984).

[25] O.Fussa, S.Kauzlarich, J.L.Dye and J.K.Teo, to be published.

[26] W.B.Fowler, "Physics of Color Centers", Academic Press, New York, (1968).

[27] P.D.Townsend, J.C.Kelly, "Colour Centers and Imperfections in Insulators and Semiconductors", Crane Russak & Company, Inc. New York, (1973).

[28] P.F.Weller, "Solid State Chemistry and Physics", Vol.I, Academic Press, New York , (1968).

[29] J.Arends and A.J.Dekker, Phys.Stat.sol 5, 265 (1964).

[30] N.H.Nachtrieb, in "Adv.Chem.Phys.", I.Prigogine and S. Rice, (eds.), Wiley, New York(1975).

[31] M.A.Bredig, Molten Salt Chem., 367(1964).

[32] N.Nicoloso and W.Freyland, J.Phys.Chem., 1977(1983).

[33] W.Freyland, K.Garbade, H.Heyer, and E.Pfeitter, J.Phys.Chem., (Colloque Weyl VI), (1983).

[34] S.Jaenicke and J.L.Dye, to be published.

[35] D.Issa, Ph.D.Dissertation, Michigan State University, (1982).

[36] G.W.Gokel, D.J.Cram, C.L.Liotta, H.P.Harris and F. L., J.Org.Chem., 39, 2445 (1974).

[37] N.Tientega, unpublished work in this lab.

[38] M.Yemen, Ph.D.Dissertation, Michigan State University, (1982).

[39] J.L.Dye and V.A.Nicely, J.Chem.educ., 48, 433 (1971).

[40] R.S.Drago, "Physical Methods in Chemistry", W.B.Saunders Company, 1977.

[41] S.G.Bratstch and J.J.Lagowski, J.Phys.Chem., 88, 1086(1974).

[42] M.Bersohn and J.C.Baird, "An introduction to Electron Paramagnetic Resonance", W.A.Benjamin, Inc.New York, 1966.

[43] E.R.Andrew, Int.Rev.Phys.Chem. 1, 195(1981).

[44] B.K.Teo and D.C.Joy, "EXAFS Spectroscopy", Plenum Press. New York, 1981.